Rational Design of the First Nonspherical Dendrimer Which Displays Calamitic Nematic and Smectic Thermotropic Liquid Crystalline Phases

Virgil Percec,*,† Peihwei Chu,† Goran Ungar,‡ and Jianping Zhou‡

Contribution from The W. M. Keck Laboratories for Organic Synthesis, Department of Macromolecular Science, Case Western Reserve University, Cleveland, Ohio 44106-7202, and the Department of Engineering Materials and Center for Molecular Materials, University of Sheffield, Sheffield S1 4D4, U.K.

Received July 24, 1995[⊗]

Abstract: The synthesis of the racemic AB_2 rodlike mesogenic monomer based on conformational isomerism, 13-hydroxy-1-(4-hydroxyphenyl)-2-(4-hydroxy-4″-*p*-terphenylyl)tridecane (**5**), and the preparation via the convergent approach of its first four generations of monodendrons and dendrimers are described. All monodendrons and dendrimers exhibit thermotropic cybotactic nematic, smectic, and crystalline phases which are generated from the *anti* conformation of the structural repeat unit derived from **5**, and therefore, they do not exhibit a spherical shape. The dependence of various transition temperatures on the generation number or on the molecular weight of these monodendrons and dendrimers follows trends similar to those of linear main chain liquid crystalline polymers containing rodlike mesogenic units. However, at similar molecular weights the viscosity of the nematic phase of these dendrimers is lower than that of the corresponding hyperbranched and linear polymers. This novel class of liquid crystalline dendrimers opens many new synthetic, theoretic, and practical opportunities in the fields of dendrimers and molecular, macromolecular, and supramolecular liquid crystals.

Introduction

Hyperbranched polymers and dendrimers are macromolecular compounds which contain a branching point in each structural repeat unit. The architecture resulting from this novel class of macromolecular compounds generates many new fundamental and technological opportunities.[1] Novel complex macromolecular architectures derived from dendrimers and/or combinations of dendrimers and other macromolecular topologies[1,2] started to become available mainly after the convergent synthetic approach to dendrimers was developed.[3] Some of the most unique characteristics of dendrimers are based on their high number of chain ends, their ability to produce spherical molecular shapes, and their inability to generate chain entanglements.[4]

We are concerned with the design of novel molecular, macromolecular, and supramolecular liquid crystals by using monodendrons, dendrimers, and hyperbranched polymers as building blocks. Two synthetic approaches are used in these experiments. The first one is based on the molecular engineering of various generations of monodendrons which exhibit a tapered shape. These monodendrons are functionalized with an endo-receptor such as a crown ether or with a polymerizable group. Upon self-assembly and/or polymerization, these taper-shaped building blocks produce a supramolecular tubular architecture which is responsible for the generation of a hexagonal columnar liquid crystalline phase.[5] The second approach is based on the design of an AB_2 monomer which yields a dendrimer that has the potential to display liquid crystallinity due to the mesogenic characters of the monomer.[6a−c] Lyotropic[6e,f] and thermotropic[6a−c,f] hyperbranched liquid crystal-

† Case Western Reserve University.

‡ University of Sheffield.

[⊗] Abstract published in *Advance ACS Abstracts*, November 1, 1995.

(1) For recent reviews and highlights on dendrimers see: (a) Service, R. F. *Science* **1995**, *267*, 458. (b) Newkome, G. R.; Moorefield, C. N. In *Mesomolecules: From Molecules to Materials*; Mendenhall, G. D., Greenberg, A., Liebman, J. F., Eds.; Chapman & Hall: New York, 1995; p 27. (c) Tomalia, D. A.; Dvornic, P. R. *Nature* **1994**, *372*, 617. (d) Fréchet, J. M. J. *Science* **1994**, *263*, 1710. (e) Vögtle, F.; Issberner, J.; Moors, R. *Angew. Chem., Int. Ed. Engl.* **1994**, *33*, 2413. (f) Tomalia, D. A. *Adv. Mater.* **1994**, *6*, 529. (g) Tomalia, D. A.; Durst, H. D. *Top. Curr. Chem.* **1993**, *165*, 193.

(2) For a few examples on the design of new complex architectures from dendrimers see: (dendrimeric box) (a) Jansen, J. F. G. A.; de Brabander-van den Berg, E. M. M.; Meijer, E. W. *Science* **1994**, *266*, 1226. (b) Jansen, J. F. G. A.; Janssen, R. A. J.; de Brabander-van den Berg, E. M. M.; Meijer, E. W. *Adv. Mater.* **1995**, *7*, 561. (well-defined micellar aggregates from dendrimers containing block copolymers). (c) Hawker, C. J.; Fréchet. J. M. J. *J. Am. Chem. Soc.* **1992**, *114*, 8405. (d) Gitsov, I.; Wooley, K. L.; Fréchet, J. M. *Angew., Chem. Int. Ed. Engl.* **1992**, *31*, 1200. (e) Hawker, C. J.; Wooley, K. L.; Fréchet, J. M. J. *J. Chem. Soc., Perkin Trans. 1* **1993**, 1287. (f) van Hest, J. C. M.; Delnoye, D. A. P.; Baars, M. W. P. L.; van Genderen, M. H. P.; Meijer, E. W. *Science* **1995**, *268*, 1592.

(3) For the convergent synthetic approach to dendritic macromolecules see: (a) Hawker, C.; Fréchet, J. M. J. *J. Chem. Soc., Chem. Commun.* **1990**, 1010. (b) Hawker. C. J.; Fréchet, J. M. J. *J. Am. Chem. Soc.* **1990**, *112*, 7638. (c) Miller, T. M.; Neenan, T. X. *Chem. Mater.* **1990**, *2*, 346.

(4) Hawker, C. J.; Farrington, P. J.; Mackay, M. E.; Wooley, K. L.; Fréchet, J. M. J. *J. Am. Chem. Soc.* **1995**, *117*, 4409.

(5) For the use of monodendrons in the self-assembly of supramolecular tubular architectures see: (a) Percec, V.; Heck, J.; Lee, M.; Ungar, G.; Alvarez-Castillo, A. *J. Mater. Chem.* **1992**, *2*, 931. (b) Percec, V.; Johansson, G.; Heck, J.; Ungar, G.; Batty, S. V. *J. Chem., Soc. Perkin Trans. 1* **1993**, 1411. (c) Percec, V.; Heck, J.; Tomazos, D.; Falkenberg, F.; Blackwell, H.; Ungar, G. *J. Chem. Soc., Perkin Trans. 1* **1993**, 2799. (d) Percec, V.; Heck, J.; Tomazos, D.; Ungar, G. *J. Chem. Soc., Perkin Trans. 2* **1993**, 2381. (e) Johansson, G.; Percec, V.; Ungar, G.; Abramic, D. *J. Chem. Soc., Perkin Trans. 1* **1994**, 447. (f) Percec, V.; Tomazos, D.; Heck, J.; Blackwell, H.; Ungar, G. *J. Chem. Soc., Perkin Trans. 2* **1994**, 31. (g) Tomazos, D.; Out, G.; Heck, J. A.; Johansson, G.; Percec, V.; Möller, M. *Liq. Cryst.* **1994**, *16*, 509. (h) Ungar, G.; Batty, S. V.; Percec, V.; Heck, J.; Johansson, G. *Adv. Mater. Opt. Electron.* **1994**, *4*, 303. (i) Kwon, Y. K.; Chvalun, S.; Schneider, A. I.; Blackwell, J.; Percec, V.; Heck, J. A. *Macromolecules* **1994**, *27*, 6129. (j) Kwon, Y. K.; Danko, C.; Chvalun, S.; Blackwell, J.; Heck, J. A.; Percec, V. *Macromol. Symp.* **1994**, *87*, 103. (k) Kwon, Y. K.; Chvalun, S. N.; Blackwell, J.; Percec, V.; Heck, J. A. *Macromolecules* **1995**, *28*, 1552. (l) Percec, V.; Heck, J.; Johasson, G.; Tomazos, D.; Ungar, G. *Macromol. Symp.* **1994**, *77*, 237. (m) Percec, V.; Heck, J.; Johansson, G.; Tomazos, D.; Kawasumi, M.; Chu, P.; Ungar, G. *J. Macromol. Sci., Pure Appl. Chem.* **1994**, *A31*, 1031, 1719. (n) Percec, V.; Heck, J.; Johansson, G.; Tomazos, D.; Kawasumi, M.; Chu, P.; Ungar, G. *Mol. Cryst. Liq. Cryst.* **1994**, *254*, 137.

0002-7863/95/1517-11441$09.00/0

Scheme 1. Structure and Dynamic Equilibrium of Different AB_2 Rodlike Monomers Based on Conformational Isomerism and of Their Corresponding Polymers Together with Their Liquid Crystalline Phase Behavior (g = glassy, n = nematic, i = isotropic)

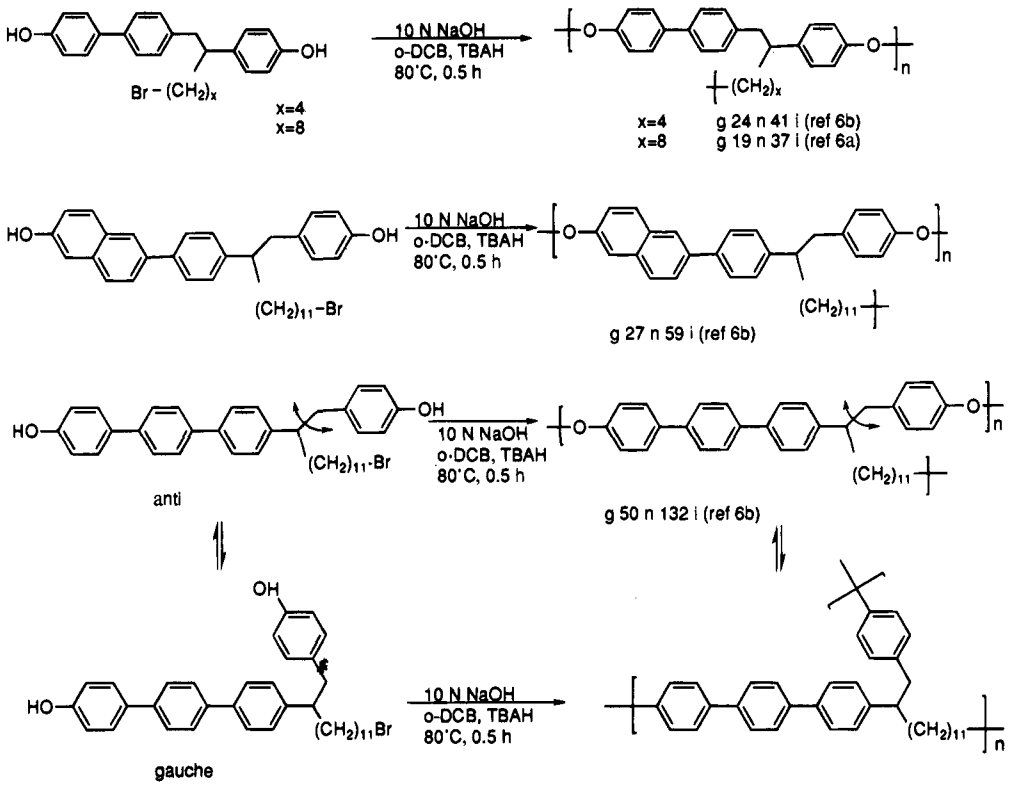

line polymers containing rodlike[6a-c] and disklike mesogens[6d] were reported recently from both our and other laboratories. Polymerization of a rodlike mesogenic AB_2 monomer yields hyperbranched polymers. The characterization of the resulting hyperbranched polymer permits the selection of the most suitable AB_2 monomer for the design of liquid crystalline dendrimers. Experiments described in two previous publications[6a,b] allowed the selection of the rodlike conformationally flexible 13-hydroxy-1-(4-hydroxyphenyl)-2-(4-hydroxy-4″-*p*-terphenylyl)-tridecane (**5**) as the optimum starting building block for the synthesis of the first examples of thermotropic liquid crystalline monodendrons and dendrimers. The goal of this paper is to describe the convergent synthesis of four generations of monodendrons and dendrimers based on **5**, as well as the characterization of their thermotropic liquid crystalline phases by a combination of techniques consisting of thermal optical polarized microscopy, differential scanning calorimetry, and X-ray diffraction experiments. **5** has a stereocenter. The experiments described here were performed with the racemic compound. These experiments will demonstrate the rational design of the first example of a dendrimer that exhibits conventional cybotactic nematic and smectic mesophases which are similar to those exhibited by classic rodlike molecular and macromolecular liquid crystals.

Results and Discussion

Scheme 1 outlines the structures of four AB_2 rodlike mesogenic monomers based on conformational isomerism which were previously reported from our laboratory.[6a,b] The dynamic equilibrium between the *anti* and *gauche* conformers of one of these monomers, the structures of the hyperbranched polymers resulting from their *anti* and *gauche* conformers, and their phase behavior are also summarized in Scheme 1.

The concept of main chain liquid crystalline polymers (LCPs) based on conformational isomerism was elaborated in our laboratory.[7] This concept allowed the molecular engineering of main chain LCPs displaying virtual, monotropic, and enantiotropic nematic,[7a-d] smectic,[7e] hexagonal columnar,[7f] and two uniaxial nematic[7g,h] mesophases as well as the elucidation of the chain conformation by small angle neutron scattering (SANS),[7i] 2D ^2H NMR,[7j,k] and dynamics by light scattering.[7l] Mesogenic monomers based on conformational isomerism were also designed for the preparation of two novel classes of liquid crystals (LCs) with complex architecture, i.e., macrocyclic[8] and hyperbranched[6a,b] polymers. The first four hyperbranched polyethers outlined in Scheme 1 exhibit a thermotropic nematic mesophase in a very narrow range of temperature.[6a,b] The

(6) For examples of thermotropic liquid crystalline hyperbranched polymers based on AB_2 rodlike monomers see: (a) Percec, V.; Kawasumi, M. *Macromolecules* **1992**, *25*, 3843. (b) Percec, V.; Chu, P.; Kawasumi, M. *Macromolecules.***1994**, *27*, 4441. (c) Bauer, S.; Fischer, H., Ringsdorf, H. *Angew. Chem., Int. Ed. Engl.* **1993**, *32*, 1589. (d) For an example of a thermotropic liquid crystalline hyperbranched polymer with disklike mesogens see: Percec, V.; Cho, C. G.; Pugh, C.; Tomazos, D. *Macromolecules* **1992**, *25*, 1164. (e) For a lyotropic liquid crystalline hyperbranched aromatic polyamide see: Kim, Y. H. *J. Am. Chem. Soc.* **1992**, *114*, 4947. (f) For a highlight on liquid crystalline hyperbranched polymers see: Kim, Y. H. *Adv. Mater.* **1992**, *4*, 764.

(7) For selected publications on main chain liquid crystalline polymers based on conformational isomerism exhibiting the characteristics in parentheses see: (nematic phase) (a) Percec, V.; Yourd, R. *Macromolecules* **1988**, *21*, 3379. (b) Percec, V; Tsuda, Y *Macromolecules* **1990**, *23*, 3509. (c) Ungar, G; Feijoo, J. L.; Keller, A.; Yourd, R.; Percec, V. *Macromolecules* **1990**, *23*, 3411. (d) Percec, V; Kawasumi, M. *Macromolecules* **1991**, *24*, 6318. (smectic phase) (e) Ungar, G.; Feijoo, J. L.; Percec, V.; Yourd, R. *Macromolecules* **1991**, *24*, 1168. (hexagonal columnar phase) (f) Ungar, G.; Feijoo, J. L.; Percec, V.; Yourd, R. *Macromolecules* **1991**, *24*, 953. (two nematic phases) (g) Ungar, G.; Percec, V.; Zuber, M. *Macromolecules* **1992**, *25*, 75. (h) Ferrarini, A.; Luckhurst, G. R.; Nordion, P. L.; Roskilly, S. J. *Chem. Phys. Lett.* **1993**, *214*, 409. (chain conformation by SANS experiments) (i) Hardouin, F.; Sigaud, G.; Achard, M. F.; Brûlet, A.; Cotton, J. P.; Yoon, D. Y.; Percec. V.; Kawasumi, M. *Macromolecules* **1995**, *28*, 5427. (conformation by 2D ^2H NMR) (j) Sherwood, M. H.; Sigaud, G.; Yoon, D. Y.; Wade, C. G.; Kawasumi, M.; Percec, V. *Mol. Cryst. Liq. Cryst.* **1994**, *254*, 455. (k) Leisen, J.; Boeffel, C.; Spiess, H. W.; Yoon, D. Y.; Sherwood, M. H.; Kawasumi, M.; Percec, V. *Macromolecules* **1995**, *28*, 6937. (dynamics by light scattering) (l) Gu, D.; Jamieson, A. M.; Kawasumi, M.; Lee, M.; Percec, V. *Macromolecules* **1992**, *25*, 2151.

Scheme 2. Synthesis of the AB_2 Building Block 13-Hydroxy-1-(4-hydroxyphenyl)-2-(4-hydroxy-4″-*p*-terphenylyl)tridecane (**5**, $\mathbf{M_1}$)

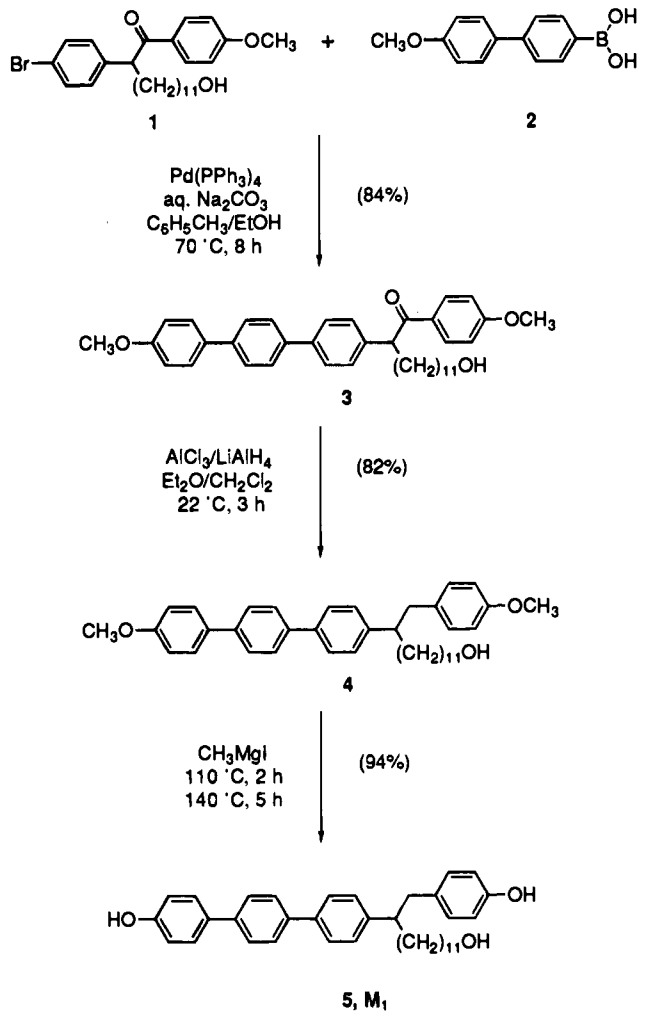

polymer obtained from 13-bromo-1-(4-hydroxyphenyl)-2-(4-hydroxy-4″-terphenylyl)tridecane displays a nematic mesophase between 50 and 132 °C. This range of temperature is suitable for physical investigations.[6b] This result contributed to our decision to use 13-hydroxy-1-(4-hydroxyphenyl)-2-(4-hydroxy-4″-*p*-terphenylyl)tridecane as the starting building block for the present investigation.

Scheme 2 outlines the synthesis of 13-hydroxy-1-(4-hydroxyphenyl)-2-(4-hydroxy-4″-*p*-terphenylyl)tridecane (**5**, $\mathbf{M_1}$) via the Suzuki cross-coupling[9] of 13-hydroxy-1-(4-methoxyphenyl)-2-(4-bromophenyl)tridecanone (**1**)[6b] with (4-methoxy-4′-biphenylyl)boronic acid (**2**)[6b] to yield 13-hydroxy-1-(4-methoxyphenyl)-2-(4-methoxy-4″-*p*-terphenylyl) tridecanone (**3**) in 84% yield. Complete reduction of the keto group of **3** with the $LiAlH_4$·$AlCl_3$·Et_2O[10] complex produced 13-hydroxy-1-(4-methoxyphenyl)-2-(4-methoxy-4″-*p*-terphenylyl)tridecane (**4**)[6b] in 82% yield. Nucleophilic demethylation of the methoxy groups of **4** with CH_3MgI[11] yielded 13-hydroxy-1-(4-hydroxyphenyl)-2-(4-hydroxy-4″-*p*-terphenylyl)tridecane (**5**) in 94% yield.

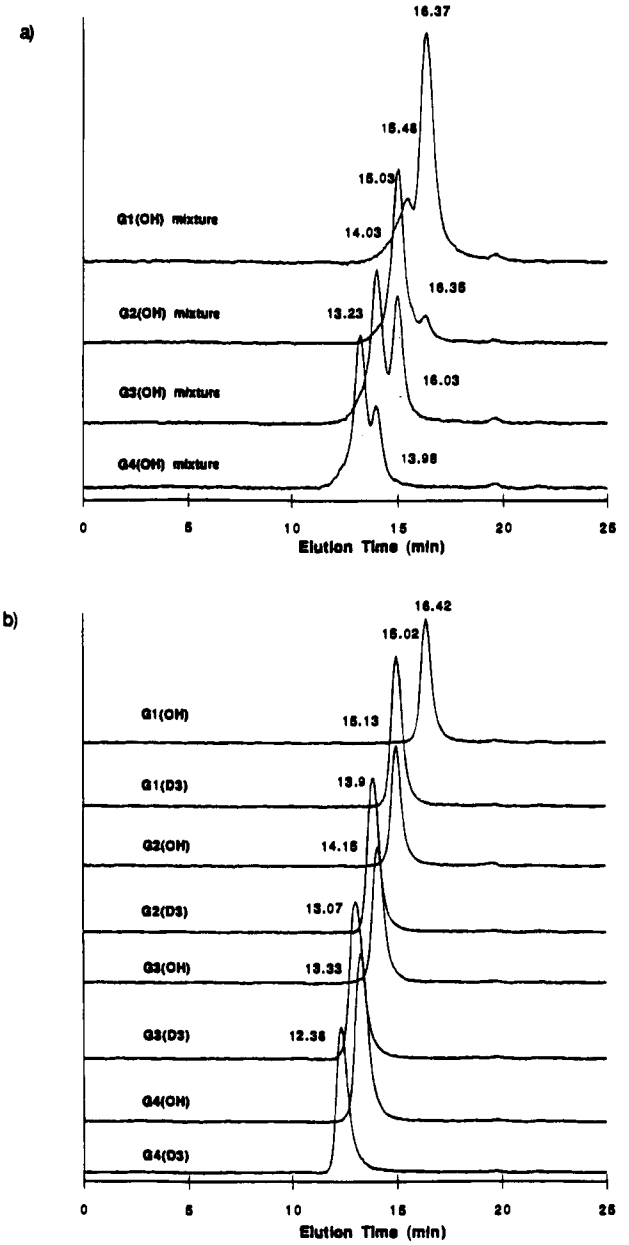

Figure 1. GPC traces of unpurified and purified $\mathbf{G_n(OH)}$ and $\mathbf{G_n(D_3)}$ ($n = 1-4$).

The synthesis of the monodendrons $\mathbf{G_n(OH)}$ ($n = 1-4$) and $\mathbf{G_n(Br)}$ ($n = 1-4$) is outlined in Scheme 3. In the first step the phenol groups of $\mathbf{M_1}$ were alkylated with 1-bromo-10-undecene in a two-phase (10 N NaOH/*o*-DCB) phase transfer catalyzed etherification with TBAH as catalyst. After purification by column chromatography (SiO_2, CH_2Cl_2), $\mathbf{G_1(OH)}$ was obtained in 80% yield. The only side product of this reaction was a small amount of the trisetherification product of $\mathbf{M_1}$. This side product was detected by ^1H NMR, TLC, and HPLC (elution time 15.48 min versus 16.37 min for $\mathbf{G_1(OH)}$) (Figure 1a). 1-Bromo-10-undecene was conveniently prepared by the reduction of 10-undecenoic acid with $LiAlH_4$ in THF[12] followed by bromination with CBr_4/PPh_3 in CH_2Cl_2.[13] Representative HPLC traces of unpurified $\mathbf{G_n(OH)}$ and purified $\mathbf{G_n(OH)}$ are presented in Figure 1. Bromination of the alcohol group of $\mathbf{G_1(OH)}$ to $\mathbf{G_1(Br)}$ was carried out with CBr_4/PPh_3 in CH_2Cl_2.[13] $\mathbf{G_1(Br)}$

(8) Macrocyclic liquid crystals: (a) Percec, V.; Kawasumi, M.; Rinaldi, P. L.; Litman, V. E. *Macromolecules* **1992**, *25*, 3851. (b) Percec, V.; Kawasumi, M. *Macromolecules* **1991**, *24*, 6318. (c) Percec, V.; Kawasumi, M. *Macromolecules* **1993**, *26*, 3663, 3917. (d) Percec, V.; Kawasumi, M. *J. Chem. Soc., Perkin Trans. 1* **1993**, 1319. (e) Percec, V. *Pure Appl. Chem.*, in press.

(9) (a) Miyaura, N.; Yanagi, T.; Suzuki, A. *Synth. Commun.* **1981**, *11*, 513. (b) Gray, G. W.; Hird, M.; Lacey, D.; Toyne, K. J. *J. Chem. Soc., Perkin Trans. 2* **1989**, 2041. (c) Hird, M.; Gray, G. W.; Toyne, K. J. *Mol. Cryst. Liq. Cryst.* **1991**, *206*, 187.

(10) (a) Nystrom, R. F.; Berger, C. R. *J. Am. Chem. Soc.* **1958**, *80*, 2896. (b) Albrecht, W. L.; Gustafson, D. H.; Horgan, S. W. *J. Org. Chem.* **1972**, *37*, 3355.

(11) (a) Hurd, C. D.; Winberg, H. E. *J. Am. Chem. Soc.* **1942**, *64*, 2085. (b) Stein, R. P.; Buzby, G. C., Jr.; Smith, H. *Tetrahedron* **1969**, *26*, 1917.

(12) Bunnell, R. H.; Shirley, D. A. *J. Org. Chem.* **1952**, *17*, 1545.

(13) Verheyden, J. P. H.; Moffatt, J. G. *J. Org. Chem.* **1972**, *37*, 2289.

Scheme 3. Synthesis of G_n(OH) and G_n(Br) (n = 1−4)

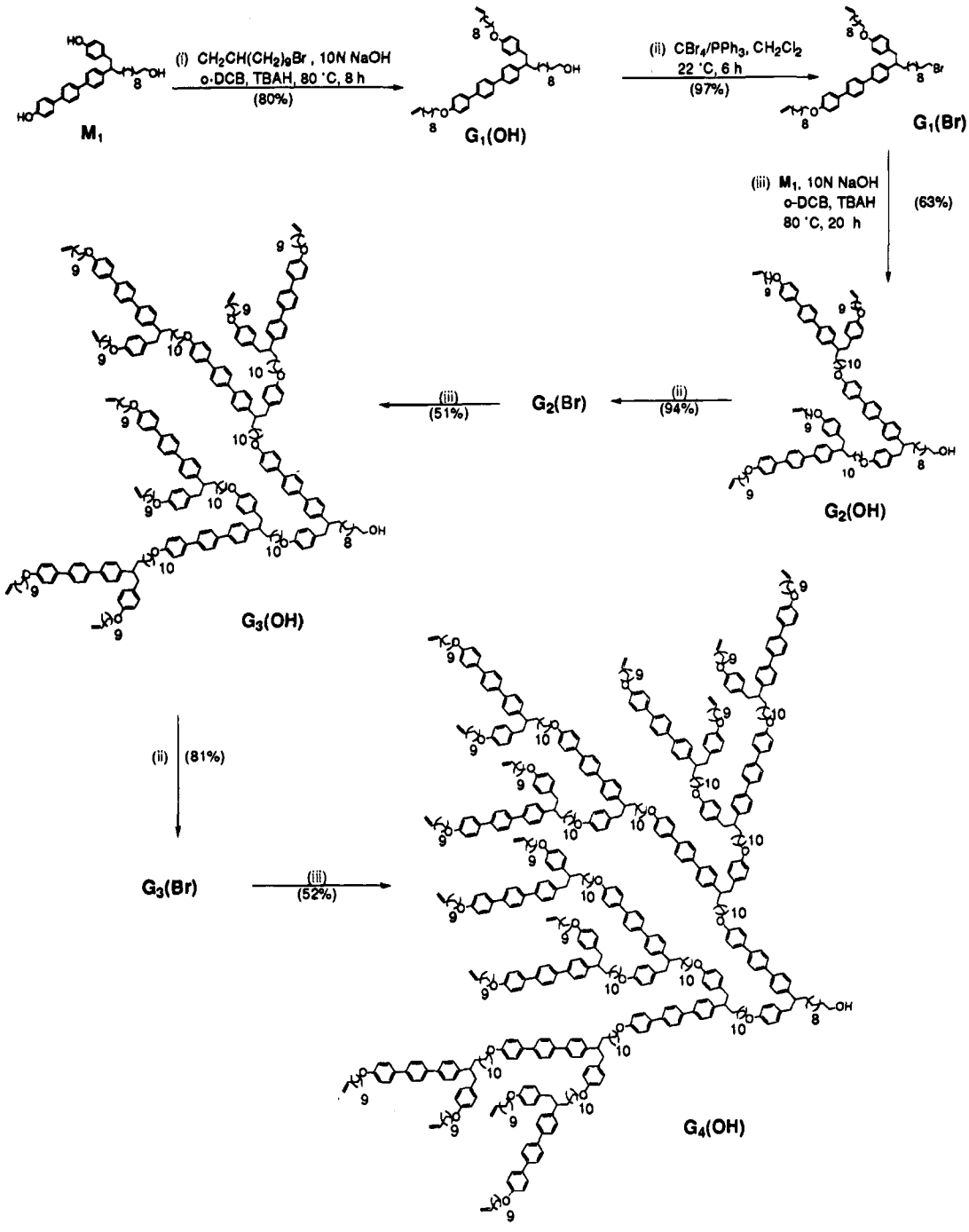

was obtained in 97% yield after purification by column chromatography (SiO_2, CH_2Cl_2/hexane).

The extent of bromination of **G_1(OH)** and the purity of **G_1(Br)** were monitored by TLC, ^{1}H NMR, and $^{13}C\{^1H\}$ NMR spectroscopy. The etherification of **M_1** with **G_1(Br)** under reaction conditions similar to those used in the synthesis of **G_1(OH)** yielded **G_2(OH)**. Bromination of **G_2(OH)** produced **G_2(Br)** (Scheme 3). The side product formed during the synthesis of **G_2(OH)** is **G_1(OH)** which is obtained by substitution at the $-CH_2Br$ group of **G_1(Br)** with OH^-. This product was detected by ^{1}H NMR, TLC, and HPLC. The HPLC trace of the unpurified **G_2(OH)** (Figure 1a) shows the presence of **G_1(OH)** at 16.35 min. **G_2(OH)** was obtained in 63% yield, while **G_2(Br)** was obtained in 94% yield. Scheme 3 also describes the alkylation of **M_1** with **G_2(Br)** to yield **G_3(OH)** which after purification by column chromatography was obtained in 51% yield. The side product obtained in this reaction is **G_2(OH)** (Figure 1a) which was produced by substitution at the $-CH_2$-Br group of **G_2(Br)** with OH^-. Bromination of **G_3(OH)** with CBr_4/PPh_3 in CH_2Cl_2 produced **G_3(Br)** in 81% yield. Alkylation of the phenol groups of **M_1** with **G_3(Br)** yielded **G_4(OH)** (Scheme 3). **G_4(OH)** was separated from the crude product in 52% yield by column chromatography. The side product of this reaction is **G_3(OH)** (Figure 1a). The GPC traces of the purified **G_1(OH)**, **G_2(OH)**, **G_3(OH)**, and **G_4(OH)** are presented in Figure 1b. The purities of **G_n(OH)** are higher than 99.5%.

The monodendrons **G_n(OH)** were esterified with 1,3,5-benzenetricarbonyl trichloride in CH_2Cl_2 by using DMAP as catalyst[14] to yield **$G_n(D_3)$** (n = 1−4, Scheme 4). The extent of this esterification reaction was monitored by TLC, NMR, and HPLC. The molar ratio between **G_n(OH)** and the tricarboxylic acid trichloride was 3/1 for **G_1(OH)** and **G_2(OH)**. A 0.3 mol excess of tricarboxylic acid trichloride was used in the esteri-

(14) (a) Kwock, E. W.; Neenan, T. X.; Miller, T. M. *Chem. Mater.* **1991**, *3*, 775. (b) Twyman, L. J.; Beezer, A. E.; Mitchell, J. C. *J. Chem. Soc., Perkin Trans. 1* **1994**, 407.

Scheme 4. Synthesis of $G_n(D_3)$ ($n = 1-4$)

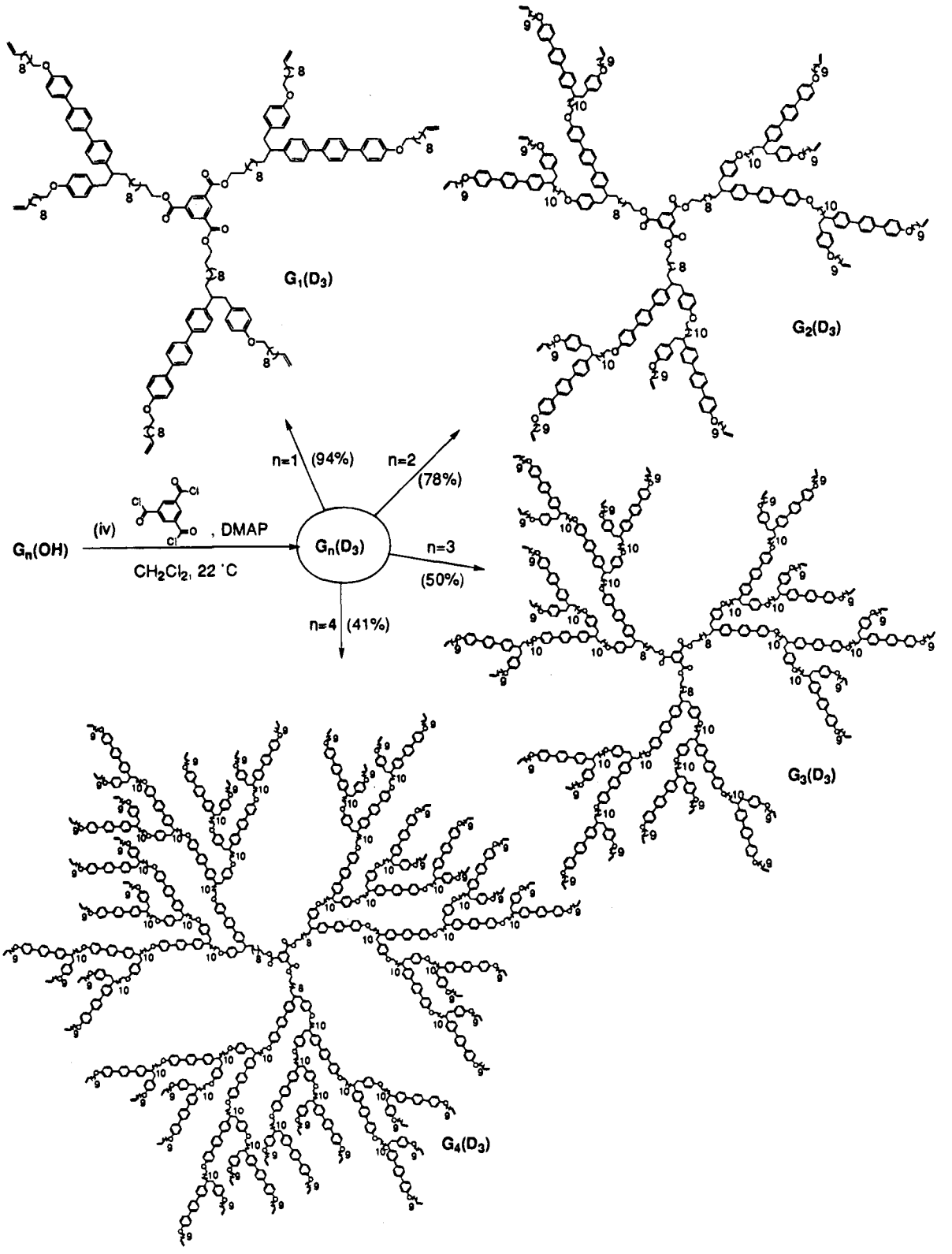

fication of G_3**(OH)** and G_4**(OH)** to complete the esterification reaction. Compounds with unreacted carboxylic acid groups were separated by column chromatography. Figure 1b shows the GPC traces of the pure monodendrons G_n**(OH)** and of the corresponding dendrimers $G_n(D_3)$. A shift toward lower elution times and higher molecular weights is obtained on going from G_1**(OH)** to G_4**(OH)**, from $G_1(D_3)$ to $G_4(D_3)$, and from G_n**(OH)** to $G_n(D_3)$.

Table 1 summarizes the theoretical molecular weights (MW_t), the relative M_n determined by GPC with polystyrene standards, the polydispersities (M_w/M_n), and the ratios M_n/MW_t for G_n**(OH)**, G_n**(Br)**, and $G_n(D_3)$. The values of M_w/M_n show that within experimental error all monodendrons and dendrimers are monodispersed products. The M_n data determined by GPC calibrated with polystyrene standards are all higher than the absolute molecular weights which are equal to MW_t. The ratio M_n/MW_t decreases especially on going from $G_1(D_3)$ to $G_4(D_3)$ and becomes almost unity for $G_4(D_3)$. This trend provides very important information. The hydrodynamic volume of monodendrons and dendrimers is higher than that of polystyrene. This difference decreases drastically in the order $G_1(D_3)$ to $G_4(D_3)$ i.e., $M_n/MW_t = 1.34$ for $G_1(D_3)$ and 1.07 for $G_4(D_3)$. These

Table 1. Theoretical and Experimental Molecular Weights and Thermal Transitions of Monodendrons G_n(OH) and G_n(Br) and Dendrimers $G_n(D_3)$[a]

G_n(X) or $G_n(D_3)$	MW_t	M_n (GPC)	M_w/M_n (GPC)	M_n/MW_t	thermal transitions (°C) and corresponding enthalpy changes (cal/g, in parentheses) heating	cooling
G_1(OH)	841.31	1293	1.04	1.54	K 66 (11.4) i	i 54 (0.16) n 46 (9.95) K
G_2(OH)	2183.34	3540	1.05	1.62	K 61 (3.08) n 92 (0.64) i g 58 S 61 (1.02) n 92 (0.70) i	i 89 (0.58) n 53 (0.92) S 41 g
G_3(OH)	4867.40	7200	1.07	1.48	K_1 58 (1.07) K_2 63 (0.03) S 69 (0.33) n 105 (0.80) i g 52 K 63 (0.05) S 69 (0.33) n 105 (0.83) i	i 102 (0.96) n 60 (0.40) S 57 (0.03) K 51 g
G_4(OH)	10235.53	14308	1.09	1.40	K 60 (0.64) S 73 (0.63) n 110 (0.94) i g 63 S 73 (0.57) n 110 (0.97) i	i 107 (0.96) n 63 (0.61) S
G_1(Br)	904.21	1252	1.04	1.38	K_1 53 (0.37) K_2 59 K_3 62 (16.63) i K_1 25 (3.56) K_2 52 (1.05) K_3 59 (14.51) i	i 58 (0.97) K_2 2 (6.25) K_1
G_2(Br)	2246.24	3168	1.06	1.41	K_1 56 K_2 58 (3.28) n 90 (0.57) i g 28 S 59 (1.03) n 90 (0.53) i	i 87 (0.54) n 45 (0.79) S
G_3(Br)	4930.30	7343	1.07	1.49	K_1 57 (1.05) K_2 65 (0.06) S 72 (0.29) n 104 (0.87) i g 49 K 65 (0.12) S 72 (0.32) n 104 (0.79) i	i 101 (0.78) n 67 (0.32) S 56 (0.07) K 49 g
$G_1(D_3)$	2680.02	3588	1.05	1.34	K 47 (4.24) n 73 (0.57) i g 5 K 32 (0.02) S 45 (0.14) n 73 (0.79) i	i 70 (0.67) n 41 (0.13) S −3 g
$G_2(D_3)$	6706.12	8679	1.07	1.29	g 36 S 51 (0.24) n 96 (0.83) i g 20 S 42 (0.06) n 96 (0.85) i	i 92 (0.86) n 18 g
$G_3(D_3)$	14758.31	17607	1.09	1.19	K 49 (0.82) S 66 (0.45) n 106 (0.98) i g 53 S 66 (0.32) n 106 (0.99) i	i 103 (0.99) n 57 (0.44) S 15 g
$G_4(D_3)$	30862.69	33118	1.09	1.07	K 49 (0.78) S 70 (0.60) n 108 (1.15) i g 49 S 70 (0.59) n 108 (1.24) i	i 105 (1.24) n 54 (0.31) S 39 g

[a] Data from the first heating and cooling are on the first line. Data from the second heating are on the second line.

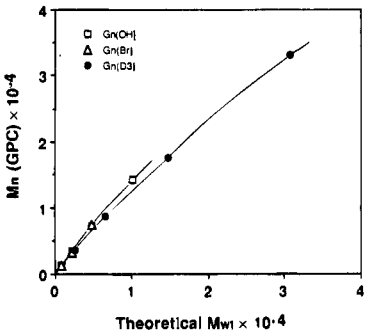

Figure 2. Dependence of M_n(GPC) vs theoretical molecular weight (MW_t) for G_n(OH) (□), G_n(Br) (△), and $G_n(D_3)$ (●).

results demonstrate that $G_n(D_3)$ are more compact than G_n(OH) and G_n(Br) and that by increasing the generation number the structure of the dendrimer becomes more compact. However, $G_n(D_3)$ are much less compact than the dendrimers with shorter distances between the branching points. Their M_n determined by GPC with polystyrene standards are lower than the corresponding theoretical values.[3b,15] Figure 2 plots the dependence of M_n on theoretical molecular weight (MW_t) for monodendrons G_n(OH) and G_n(Br) and dendrimers ($G_n(D_3)$). These plots indicate that monodendrons and dendrimers represent two different classes of polymers. The same information is obtained by following both the ^{1}H NMR and $^{13}C\{^1H\}$ NMR spectra of G_n(OH), G_n(Br), and $G_n(D_3)$ as a function of the generation number. The chemical shifts of both proton and carbon resonances of the present monodendrons and dendrimers are not affected by their size. Figure 3a shows the $^{13}C\{^1H\}$ NMR spectra of G_1(OH) and G_4(OH) while Figure 3b shows the spectra of $G_1(D_3)$ and $G_4(D_3)$. However, in the case of more dense dendrimers the chemical shifts of their resonances are strongly dependent on the generation number.[16]

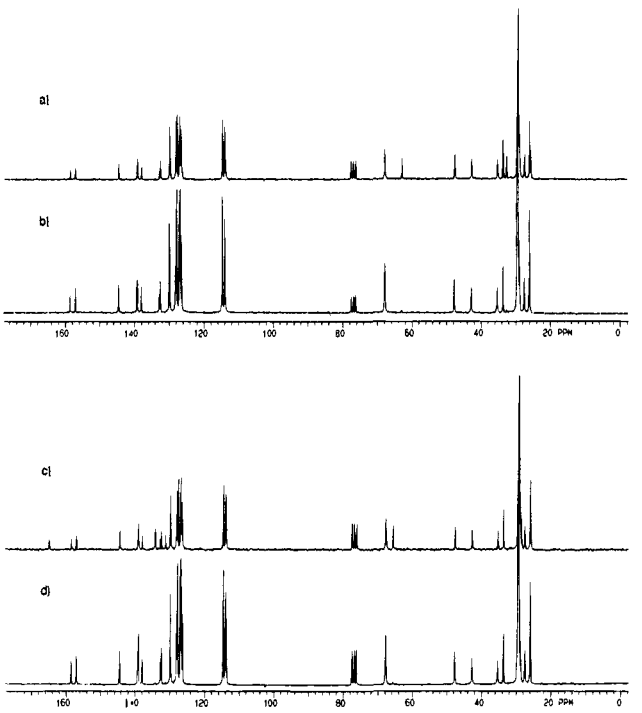

Figure 3. 50 MHz $^{13}C\{^1H\}$ NMR spectra of (a) G_1(OH), (b) G_4(OH), (c) $G_1(D_3)$, and (d) $G_4(D_3)$ ($CDCl_3$). Chemical shift assignments are available in the supporting information.

Thermal behavior of all monodendrons G_n(OH) and G_n(Br) and dendrimers $G_n(D_3)$ was characterized by a combination of differential scanning calorimetry (DSC) and thermal optical polarized microscopy. The structures of various phases were assigned by X-ray diffraction experiments which will be discussed later. Figure 4a presents second heating and Figure 4b first cooling DSC traces of G_n(OH). G_n(Br) exhibits DSC traces almost identical with those of G_n(OH), and these traces are not shown. Phase transition temperatures and corresponding thermodynamic parameters collected from first and second heating scans and from the cooling scans are summarized in Table 1. It is instructive to follow the trend observed in Figure 4. On heating, G_1(OH) displays a melting and, on cooling, a

(15) (a) Hawker, C. J.; Fréchet, J. M. J. *Macromolecules* **1990**, *23*, 4726. (b) Xu, Z.; Kahr, M.; Walker, K. L.; Wilkins, C. L.; Moore, J. S. *J. Am. Chem. Soc.* **1994**, *116*, 4537.

(16) (a) Wooley, K. L.; Hawker, C. J.; Fréchet, J. M. J. *J. Chem. Soc., Perkin Trans. 1* **1991**, 1059. (b) Wooley, K. L.; Hawker, C. J.; Fréchet, J. M. J. *J. Am. Chem. Soc.* **1991**, *113*, 4252. (c) Morikawa, A.; Kakimoto, M.; Imai, Y. *Macromolecules* **1993**, *26*, 6324.

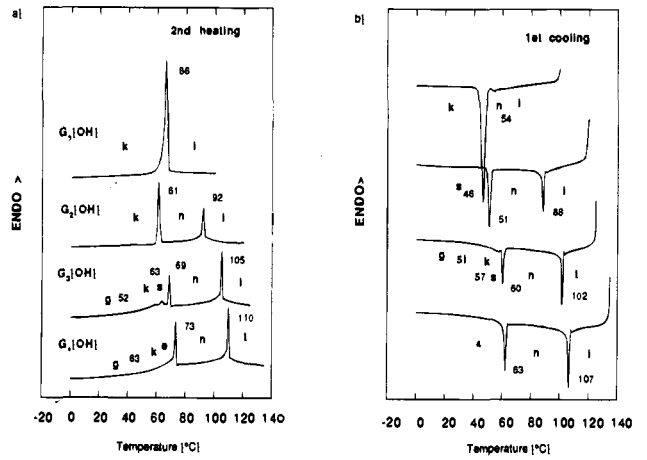

Figure 4. Second heating (a) and first cooling (b) DSC traces of G_n-(OH) (n = 1−4).

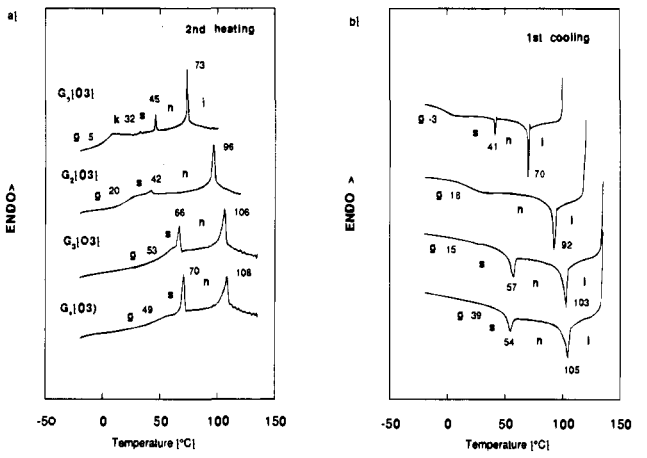

Figure 5. Second heating (a) and first cooling (b) DSC traces of $G_n(D_3)$ (n = 1−4).

very narrow nematic phase followed by crystallization. Therefore, **G_1(OH)** displays only a monotropic nematic mesophase. **G_1(Br)** is only crystalline (Table 1). The formation of the nematic phase in **G_1(OH)** may be favored by H-bonding between −OH groups. **G_2(OH)** exhibits a crystalline phase followed by an enantiotropic nematic phase. Both **G_3(OH)** and **G_4(OH)** display a crystalline phase followed by enantiotropic nematic and smectic mesophases. Therefore, by increasing the generation number from **G_1(OH)** to **G_4(OH)**, a higher tendency toward the formation of liquid crystalline phases and a lower rate of crystallization are observed. The isotropization temperature of the nematic phase and the smectic−nematic transition temperature both increase with the generation number. Monodendrons **G_n(Br)** follow the same trend as **G_n(OH)**. During the first heating scan more perfect crystalline phases than during the second one are observed, and at low generation numbers crystallization occurs in the smectic phase.

The trends observed in Figure 4, i.e., an increase of the isotropization temperature and the formation of new mesophases at higher molecular weights, are well established in the field of main chain and side chain liquid crystalline polymers,[17,18] and are explained by thermodynamics.[19]

Figure 5 presents the second heating and first cooling DSC traces of **$G_n(D_3)$**. The transformation of **G_1(OH)** into **$G_1(D_3)$** changes the monotropic nematic phase of **G_1(OH)** into an enantiotropic one and in addition creates a smectic phase in **$G_1(D_3)$**. This trend is consistent with the trend observed upon the increase of molecular weight in the series of monodendrons **G_1(OH)** to **G_3(OH)** (Figures 4 and 5). However, the isotropization temperature of **$G_1(D_3)$** is lower than that of **G_2(OH)** although their molecular weights are similar. This means that although the transition from **G_n(OH)** to **$G_n(D_3)$** favors the formation of liquid crystalline phases, the corresponding increase of the transition temperature is less on going from monodendrons to dendrimers than that observed by increasing the generation number of the monodendrons. This trend might be associated with the fact that the architecture provided by **G_n-(D_3)** is less favorable than that provided by **G_n(OH)** for the formation of the liquid crystalline phase. The remaining DSC traces in Figure 5 are self-explanatory. A general increase of the smectic−nematic and nematic−isotropic transition temperatures by increasing the size of the dendrimers is observed.

It is extremely instructive at this point to follow the plots of various transition temperatures of **G_n(OH)** and **$G_n(D_3)$** as a function of n (i.e., n is the number of structural repeat units) and respectively their theoretical molecular weight (MW_t). These plots demonstrate the clear trend that the transition temperatures of **G_n(OH)** and **$G_n(D_3)$** follow two different sets of curves. This trend is consistent with the one observed in Figure 2. The plots in Figure 6b,c seem to be the most meaningful. The isotropic−nematic transition temperature has a higher slope for the case of **G_n(OH)** than for **$G_n(D_3)$**, and therefore, it reaches a plateau at much lower molecular weights than the corresponding **G_n-(D_3)**. The trend in Figure 6 resembles well-established trends from the field of conventional liquid crystalline polymers.[18,19] Figure 7 plots the enthalpy changes associated with various phase transition temperatures of **G_n(OH)**, **G_n(Br)**, and **$G_n(D_3)$** as a function of the generation number n (Figure 7a) and their number of repeat units (Figure 7b). Once again monodendrons and dendrimers follow two different curves. In the case of side chain liquid crystalline polymers these values are independent of molecular weight.[20a] However, in the case of main chain liquid crystalline polymers they follow a trend similar to that in Figure 7.[20b,c] From this point of view, dendrimers and monodendrons resemble, as expected, main chain liquid crystalline polymers.

Another interesting characteristic of this novel class of liquid crystalline polymers is the sharpness of their transition peaks and their very low degrees of supercooling, observed even at very high molecular weights on the DSC traces (Figures 4 and 5).

On the thermal optical polarized microscope **G_n(OH)**, **G_n-(Br)**, and **$G_n(D_3)$** exhibit textures which are similar to those displayed by calamitic mesophases of classic rodlike mesogens.[21] Figure 8 presents selected textures of the nematic phase of **G_2(OH)**, **G_4(OH)**, **$G_1(D_3)$**, and **$G_2(D_3)$**. It is note-

(17) For a few examples of side chain LCPs which display more mesophases at high molecular weights see: (a) Percec, V.; Oda, H.; Rinaldi, P. L.; Hensley, D. R. *Macromolecules* **1994**, *27*, 12. (b) Percec, V.; Oda, H. *Macromolecules* **1994**, *27*, 4454, 5821.

(18) For general reviews on main chain and side chain LC polymers which show different trends of phase transition temperatures−molecular weight dependence see: (a) Percec, V .; Pugh, C. In *Side Chain Liquid Crystalline Polymers*; McArddle, C. B., Ed.; Chapman and Hall: New York, 1989; p 30. (b) Percec, V.; Tomazos, D. In *Comprehensive Polymer Science*, First Suppl.; Allen, G., Ed.; Pergamon: Oxford, 1992; p 299. (c) Percec, V.; Tomazos, D. *Adv. Mater.* **1992**, *4*, 548. (d) Percec, V. In *Handbook of Liquid Crystal Research*; Collings, P. J., Patel, J. S., Eds.; Oxford University Press: Oxford, in press.

(19) For thermodynamic schemes which explain the dependence of liquid crystalline transitions on molecular weight see: (a) Percec, V.; Keller, A. *Macromolecules* **1990**, *23*, 4347. (b) Keller, A.; Ungar, G.; Percec, V. In *Advances in Liquid Crystalline Polymers*; Weiss, R. A., Ober, C. K., Eds.; ACS Symposium Series 435; American Chemical Society: Washington, DC, 1990; p 308.

(20) For the dependence of thermodynamic parameters of phase transitions on molecular weight in liquid crystal polymers see: (side chain) (a) Percec, V.; Tomazos, D.; Pugh, C. *Macromolecules* **1989**, *22*, 3259. (main chain) (b) Percec, V.; Nava, H.; Jonsson, H. *J. Polym. Sci., Polym. Chem. Ed.* **1987**, *25*, 1943. (c) Percec, V.; Kawasumi, M. *Macromolecules* **1993**, *26*, 3663.

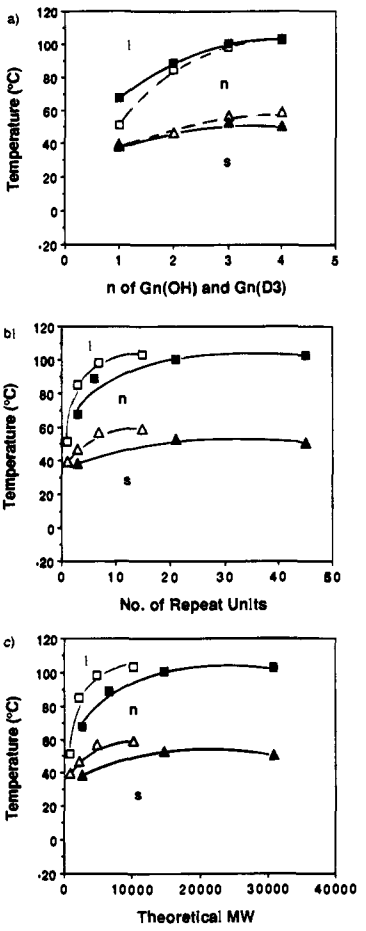

Figure 6. Dependence of various transition temperatures of G_n(OH) and $G_n(D_3)$ on (a) generation number n, (b) number of repeat units, and (c) theoretical molecular weight (MW_i). In all cases data are from the first DSC cooling scan. Symbols always have the same meaning, i.e., for G_n(OH) △ = T_{n-s} or T_{n-k} and □ = T_{i-n} and for $G_n(D_3)$ ▲ = T_{n-s} or T_{n-k} and ■ = T_{i-n}.

worthy that the molecular weight of $G_4(D_3)$ (30862.69) is the highest of any known molecular liquid crystal. In spite of this, its viscosity is very low and the texture of its nematic phase forms very fast (i.e., at a comparable rate with the texture formed by low molar mass liquid crystals). Similar main chain liquid crystalline polyethers with $M_n \cong 30000-40000$ are not able to form textures similar to those of low molar mass liquid crystals and can be aligned in magnetic or in electric fields only with great difficulty.[7i,j] This very interesting behavior is completely different from that of linear high molecular weight and even of hyperbranched[6a,b] polymers.

The next obvious question is what the molecular arrangement of the structural repeat units is in both monodendrons and dendrimers in their liquid crystalline phase. Are the repeat units in their *anti* or in their *gauche* conformation? The *gauche* conformation of the repeat unit yields monodendrons and dendrimers with the architectures presented in Schemes 2 and 3. It is impossible to envision a nematic director for these structures. In the liquid crystalline phase main chain liquid crystalline polymers with mesogenic units based on conformational isomerism have their mesogens in the *anti* conformation.[7i-k]

Scheme 5 outlines the alternative structures of G_2(OH), G_3(OH), and G_4(OH) which are based on the *anti* conformer of the monomeric repeat unit and also illustrates the dynamic

(21) (a) Demus, D.; Richter, C. *Textures of Liquid Crystals*; Verlag Chemie: Weinheim, 1978. (b) Gray, G. W.; Goodby, J. W. *Smectic Liquid Crystals. Textures and Structures*; Leonad Hill: Glasgow, 1984.

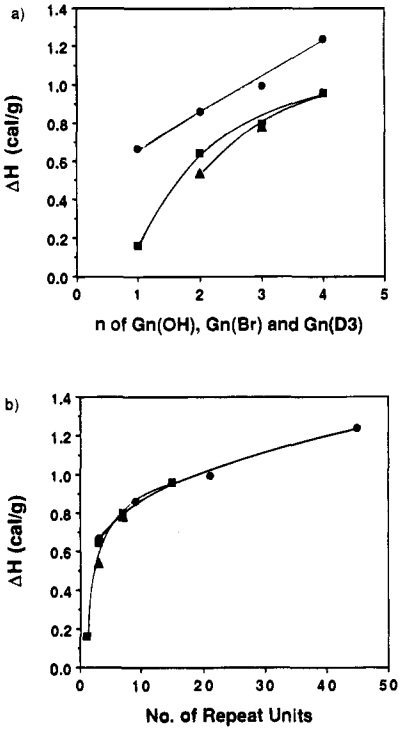

Figure 7. Dependence of enthalpy changes (ΔH, cal/g) associated with isotropic–nematic transition temperatures of G_n(OH) (■), G_n(Br) (▲), and $G_n(D_3)$ (●) plotted as a function of generation number n (a) and number of repeat units (b).

equilibrium between the *gauche* and *anti* conformers for G_2(OH). X-ray diffraction experiments were carried out to obtain information about the structure of G_n(OH) and $G_n(D_3)$ in their nematic and smectic phases. These experiments were performed on samples which were preoriented in glass capillaries in a 1 T field of a heated cell. All G_n(OH) and $G_n(D_3)$ samples studied show a large number of common features. In all cases the higher temperature mesophase is nematic. Reasonable alignment of all monodendrons and dendrimers can be achieved even with this moderate magnetic field of 1 T. Surprisingly, the $G_n(D_3)$ dendrimers align better than their lower molecular weight G_n(OH) counterparts. The scattering pattern of $G_1(D_3)$ is shown in Figure 9a. The patterns obtained from the nematic phase of samples $G_1(D_3)$ to $G_4(D_3)$ is similar to that in Figure 9a and show intense diffuse low-angle scattering in the form of a layer-line streak with off-meridional maxima (the meridian and equator are defined with respect to the unique axis, which in this and subsequent figures is horizontal). This low-angle scatter indicates the existence of strong smectic-C type fluctuations. Such a nematic phase is sometimes referred to as cybotactic.[22] The layer-line spacing of the nematic phase corresponds to 45 ± 1 Å for $G_1(D_3)$ and 49 ± 1 Å for $G_2(D_3)$.

On cooling below the nematic temperature range, a smectic phase forms which as observed by DSC and optical polarized microscopy is in some cases metastable. It is particularly unstable in the first generation $G_1(D_3)$, giving way with time to a low-symmetry crystalline form. A typical pattern of the oriented smectic phase is shown in Figure 9b. This example is for $G_2(D_3)$ at 33 °C. The low-angle region is dominated by four orders of diffraction from tilted layers of periodicity d = 84.1 ± 0.6 Å. The tilt angle between the layer normal and magnetic field direction is $\alpha/2 = 30°$. This gives the layer periodicity along the field direction as $d_m = d/\cos 30° = 97$ Å. The wide angle region is dominated by a single sharp diffraction maximum of Lorentzian line shape, corresponding to a Bragg spacing of 4.465 Å. The diffuse scattering at the bottom of the

(22) de Vries, A. *Mol. Cryst. Liq. Cryst.* **1970**, *10*, 219.

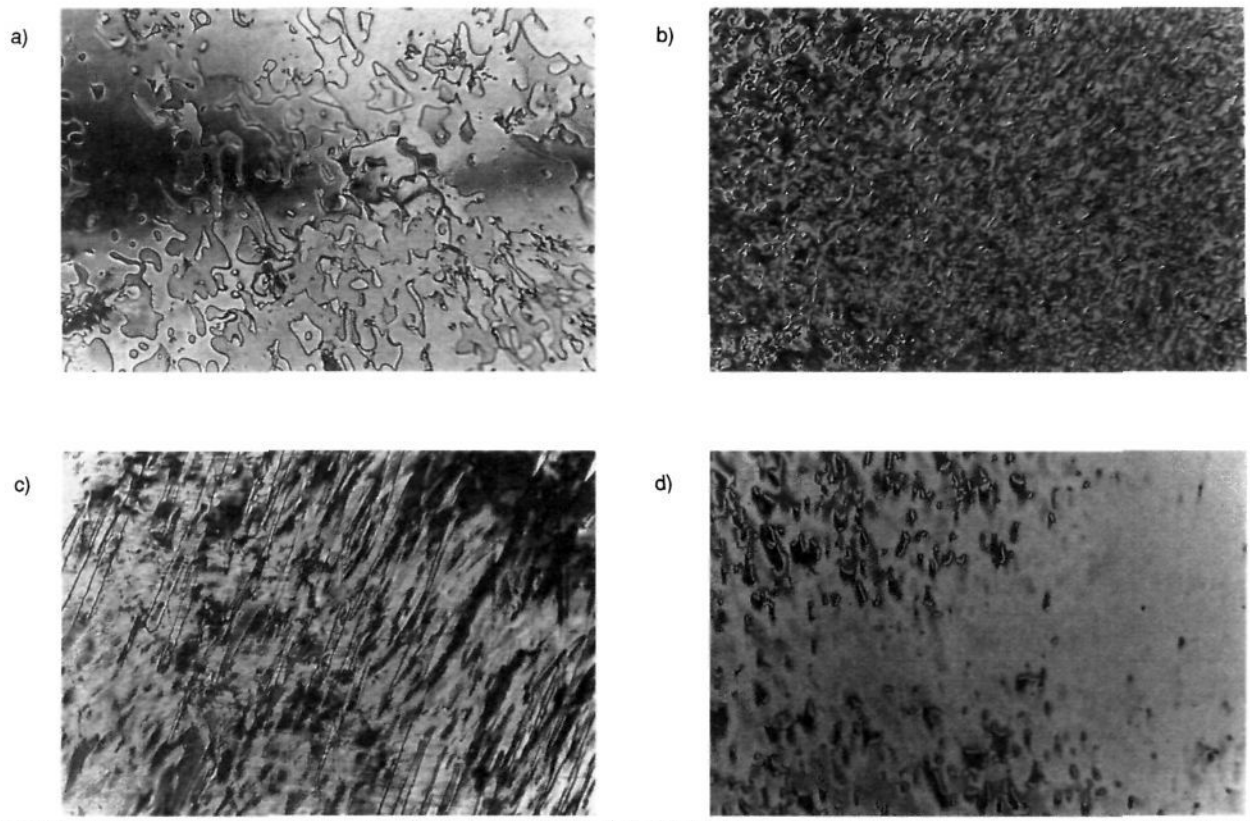

Figure 8. Representative textures exhibited by the nematic phase of (a) **G_2(OH)** at 89 °C, (b) **G_4(OH)** after 30 min at 107 °C, (c) **$G_1(D_3)$** after 10 min at 73 °C, and (d) **$G_2(D_3)$** after 10 min at 96 °C.

Scheme 5. Dynamic Equilibrium between the Structures of **G_2(OH)** Resulting from *gauche* and *anti* Conformers of Their Structural Repeat Units and the Structure of **G_2(OH)**, **G_3(OH)**, and **G_4(OH)** Obtained with Their Structural Units in the *anti* conformation

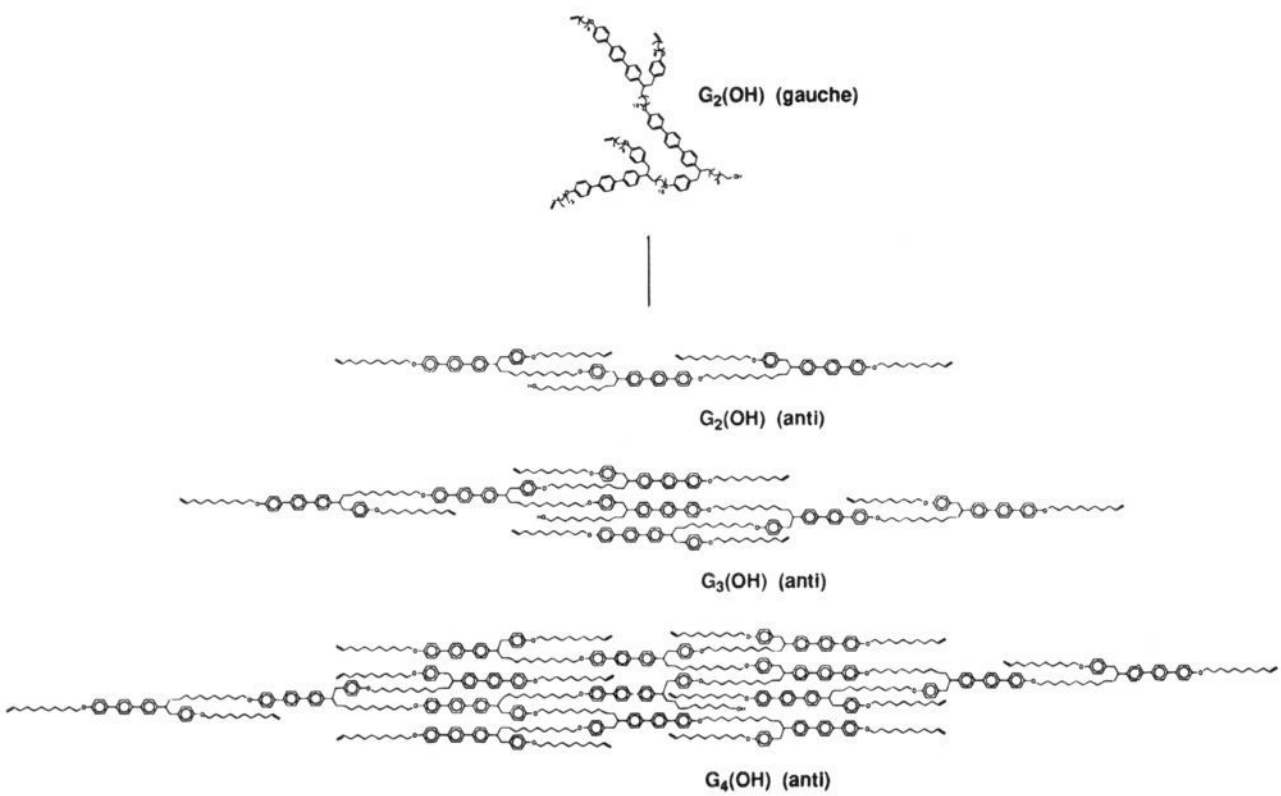

peak is seen as broad black areas in the "overexposed" pattern of Figure 9b. As the "underexposed" pattern in Figure 9c shows, the sharp 4.465 Å arcs are in fact split azimuthally, the maxima making an angle of $\beta/2 = 17°$ with the equator.

The smectic phase is similar in all dendrimeric compounds studied. Figure 9d shows the diffraction pattern of the almost randomly oriented smectic phase in **G_2(OH)**. Apart from exhibiting a lower tendency to align in the magnetic field, other

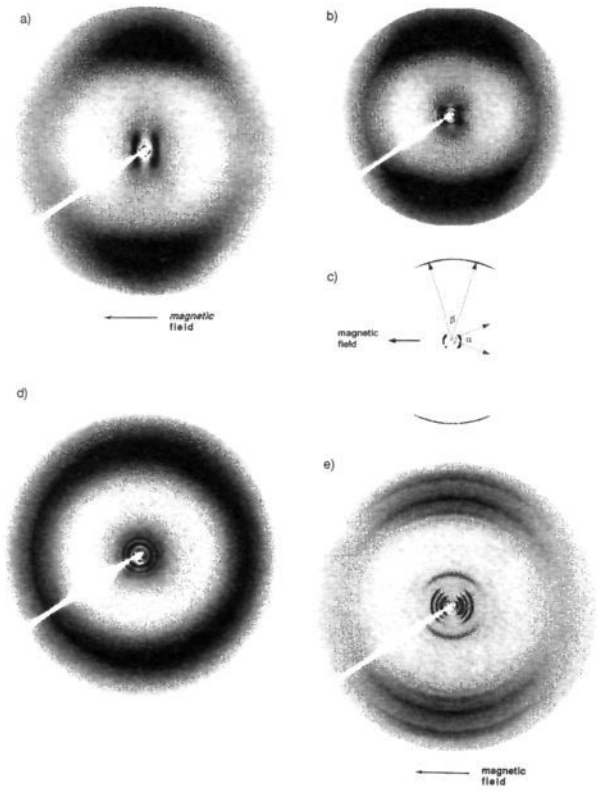

Figure 9. (a) X-ray diffraction pattern of $G_1(D_3)$ in the nematic phase at 57 °C. (b) X-ray diffraction pattern of the smectic phase of $G_2(D_3)$ recorded at 33 °C (full gray scale). (c) X-ray diffraction pattern of the smectic phase of $G_2(D_3)$ recorded at 33 °C (clipped gray scale (high contrast) pattern). (d) X-ray diffraction pattern of the smectic phase of G_2(OH) recorded at room temperature. (e) X-ray diffraction pattern of the crystalline phase of $G_1(D_3)$ recorded at room temperature. The sample was crystallized in the magnetic field by cooling from the isotropic melt through the nematic and smectic phases.

characteristics of the phase are qualitatively the same as those of the smectic phase in $G_2(D_3)$. Here the four diffraction orders correspond to a layer periodicity of 81.5 ± 1 Å. Compared to this value is the practically identical spacing of 81.7 ± 0.5 Å for G_4(OH), and the slightly larger values of 84.1 and 83.5 Å for $G_2(D_3)$ and $G_3(D_3)$, respectively. In spite of the poor alignment of the smectic phase in the G_1(OH) compounds there are indications that the layers are tilted also in this case. The latter is deduced from the observation that a relatively well aligned nematic phase apparently loses orientation as it transforms into the smectic phase, but regains its initial alignment almost completely upon subsequent heating to the nematic state. The molecular directors must have preserved their orientation throughout the described cycle.

On the basis of the diffraction data presented above the smectic phase can be best described as Sm-J or Sm-G. These are the two phases with hexagonal in-plane order and the director tilted, respectively, toward an apex or a side of the basal hexagon. In principle, both of these phases have three-dimensional positional long-range order. At present, however, we do not completely rule out the analogous hexatic versions, Sm-I or Sm-F, although the narrow line width of the 4.5 Å diffraction maximum suggests that this is a true Bragg reflection. It may prove impossible in this case to distinguish between an imperfect crystal and a genuinely hexatic smectic phase. The fact that *hkl* reflections, expected in Sm-J or G, are not observed in the current diffraction patterns causes ambiguity in the phase assignment.

Figure 9e shows the diffraction pattern of the crystalline phase in $G_1(D_3)$ formed by cooling from the aligned nematic melt

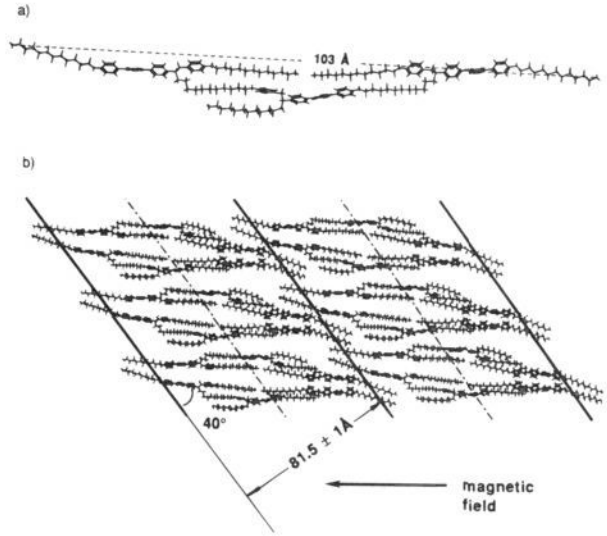

Figure 10. (a) Molecular model of the extended conformation of G_2(OH). The end-to-end distance is 103 Å. (b) Schematic model of the molecular arrangement in the smectic phase of G_2(OH) built from the molecular model from (a). The magnetic field is nearly horizontal. For further explanation see the text.

and via the smectic phase. As in the smectic phase, the low-angle region is characterized by four orders of diffraction from tilted layers. This time the Bragg spacing is d = 91.7 Å, as compared to the smectic periodicities of 84.1 and 83.5 Å for $G_2(D_3)$ and $G_3(D_3)$. The tilt angle is 27°. In addition to these layer reflections, a relatively strong arc centered at the equator is observed in the lower angle portion of the diffraction pattern; it corresponds to a spacing of 14.7 Å.

Attempts were made at relating the observed X-ray diffraction features to molecular models. The fact that compounds with disparate shapes and sizes give diffraction patterns of considerable similarity indicates that the liquid crystal phases in question are governed by the same principal mode of packing involving the same or similar subunits. The two recurring structural features are tilted layers and a periodicity of between 90 and 100 Å along the director for the smectic phase, the scale of short-range fluctuations in the nematic phase being half this value. A basic molecular conformation which appears to be qualitatively compatible with most of these observations is the *anti* extended *"windscreen wiper"* conformation of G_2(OH) shown in Figure 10a. The three monomeric repeat unit moieties are all in the extended trans (*anti*) conformation, as would be expected from their mesogenic properties. The molecule has an overall elongated shape with an end-to-end distance of 103 Å in its most extended form. The tendency for tilting is believed to be a consequence of the expected lack of rotational freedom around the long axis of the dendritic molecule due to steric hindrance. Thus, symmetry breaking through molecular tilt is not significantly disfavored entropically.

The large discrepancy between cross sections of the middle and the end sections of the molecule (see Figure 10a) would favor interdigitation, and an arrangement where thick central portions and thin end portions of adjacent molecules alternate is one possible candidate for consideration. However, this is most likely to lead to halving of the layer periodicity, i.e., from one on the order of 100 Å to one on the order of 50 Å. Such an arrangement would also be disfavored in a smectic phase as molecules would straddle adjacent layers. Indeed, as shown by X-ray diffraction, the layer periodicity along the director is on the order of 100 Å. It is noteworthy, however, that the second-order diffraction intensity is significantly higher than that of the first-order diffraction, which may point to a

considerable number of straddling molecules. We also note that in the nematic phase diffuse scattering is observed only in the 50 Å range, indicating the probable existence of a staggered local arrangement of molecules as described above.

A schematic diagram of the proposed molecular arrangement in the smectic phase of **G_2(OH)** monodendrons is shown in Figure 10b. The high degree of order is not meant to represent true translational periodicity, but rather to illustrate the underlying symmetry of the system. Molecules are shown in pairs to depict the C_2 symmetry. We note that the *"root"* alkoxy chain is more likely to bend toward the phenyl group and away from the terphenyl group. This causes considerable molecular asymmetry which is, we believe, important in determining the tilt angle. The structure in Figure 10b reconciles the tendencies for both space filling and molecular layer separation. The tilt angle (angle between layer normals and the molecular director) is ca. 40° in Figure 10b, compared to ca. 30° observed experimentally. The actual tilt angle will depend on detailed molecular geometry and will be reduced to some extent by partial axial rotational averaging of the molecules.

In broad agreement with the model is the observed lateral periodicity of 14.7 Å observed in the crystalline phase of **G_1(D_3)**. This value should be compared with the 30.6 Å translation between molecular pairs along the layer in Figure 10b or the 15.3 Å average separation between individual molecules in the same direction. The high intensity of the second low-angle diffraction order can be partially due to the already mentioned proportion of straddling molecules halfway between the layers. However, since even orders are also dominant in the more ordered crystalline phase (Figure 9e), we believe that the reason lies in the molecular structure itself. We note that chain ends are concentrated not only at the layer boundaries, but also in the center of the layers (dot−dash line in Figure 10b). This would result in an additional electron density minimum halfway across the layer profile. This gap causing the second minimum is expected to be larger than suggested in Figure 10b due to thermal contraction of the adjoining alkoxy chains.

Models of **G_1(D_3)** and **G_2(D_3)** molecules suggest a similar type of packing as that suggested here for **G_2(OH)**. In the case of the longer third and fourth generations of dendrimers a 100 Å layer smectic phase cannot be explained in terms of extended molecules separated into individual layers. Either the molecules fold or glide plane-type extinction of a fundamental long period occurs due to interdigitation. These questions will be addressed in further studies.

In conclusion, the racemic AB_2 rodlike building block based on conformational isomerism, 13-hydroxy-1-(4-hydroxy-phenyl)-2-(4-hydroxy-4″-*p*-terphenylyl)tridecane (**5**), was used in the convergent synthesis of four generations of monodendrons (**G_n(OH)** and **G_n(Br)**) and dendrimers (**G_n(D_3)**). These are the first examples of dendrimers which display conventional calamitic cybotactic nematic and smectic liquid crystalline phases. The corresponding hyperbranched polymers exhibit only a nematic phase and do not crystallize.[6b] Also, the viscosity of the nematic phase of hyperbranched and linear polymers of similar molecular weights is much higher than that of the present monodendrons and dendrimers. In addition, in the nematic phase the viscosity of dendrimers is lower than the viscosity of monodendrons, and therefore, the alignment of dendrimers in a magnetic field is faster than that of the monodendrons. Due to their design, the liquid crystalline phases of the monodendrons and dendrimers are generated from the *anti* conformation of the structural repeat unit derived from **5**. Therefore, in their liquid crystalline and crystalline phases the first four generations of these monodendrons and dendrimers do not have a spherical shape. ^{1}H and ^{13}C{^{1}H} NMR and GPC experiments suggest that these dendrimers do not exhibit a very compact shape even in solution. The behavior of these compounds in solution and the melt phase is determined by the conformational flexibility of the building block used in their synthesis and the long spacer connecting the structural repeat units. We expect that at higher generations these dendrimers will approach a spherical shape which will not favor the formation of the liquid crystalline phase. These dendrimers represent a novel class of liquid crystalline materials[18,23] which yield many new synthetic, theoretic, and technologic opportunities derived from their high number of chain ends per molecule (for example, **G_4(D_3)** has 48 chain ends) and low melt viscosity in the nematic phase. New molecular, macromolecular, and supramolecular architectures derived from these racemic and chiral monodendrons and dendrimers and from their higher generations as well as from the functionalization of their chain ends are under investigation.

Experimental Section

Materials. $LiAlH_4$ (95+%), $AlCl_3$ (anhydrous), tetrabutylammonium hydrogen sulfate (TBAH, 97%), BH_3·THF (1.0 M in THF), PPh_3 (99%), CBr_4 (99%), 1,3,5-benzenetricarbonyl trichloride (98%) (all from Aldrich), Na_2CO_3, K_2CO_3, CH_3I (99%) (all from Fisher Scientific), Mg, 10-undecenoic acid (both from Fluka), and 4-(dimethylamino)pyridine (DMAP) (from Lancaster) were used as received. Et_2O was dried by refluxing over $LiAlH_4$ followed by distillation. CH_2Cl_2 and $CHCl_3$ were refluxed over CaH_2 and distilled before use. THF was dried by refluxing on Na−benzophenone and was freshly distilled before use. *o*-Dichlorobenzene (*o*-DCB) was distilled under reduced pressure. 13-Hydroxy-1-(4-methoxyphenyl)-2-(4-methoxy-4″-*p*-terphenylyl)tridecanone (**3**) and 3-hydroxy-1-(4-methoxyphenyl)-2-(4-methoxy-4″-*p*-terphenylyl)tridecane (**4**) were prepared by previously published methods.[6b] 10-Undecen-1-ol[12] (**7**) was prepared by a modified literature procedure in which 10-undecenoic acid was reduced with $LiAlH_4$ in THF. 1-Bromo-10-undecene (**8**) was prepared by a modified literature procedure in which **7** was brominated with CBr_4/PPh_3.[13] All other chemicals were commercially available and were used as received.

Techniques. ^{1}H NMR (200 MHz) and ^{13}C{^{1}H} NMR (50.2 MHz) spectra were recorded on Varian XL-200 and Gemini spectrometers with TMS as the internal standard in $CDCl_3$ or acetone-d_6 solution. The purity of the products was determined by a combination of thin layer chromatography (TLC) on silica gel plates (Kodak) with a fluorescent indicator and high-pressure liquid chromatography (HPLC). GC analyses were performed on an HP 5890 gas chromatograph using a flame ionization detector and 10% SP-2100 column. Melting points were determined with a capillary melting point apparatus (powder sample) or a Perkin-Elmer DSC-7 (solid sample). Relative molecular weights of the monodendrons and dendrimers were determined by gel permeation chromatography (GPC). HPLC and GPC analyses were accomplished with a Perkin-Elmer Series 10 LC equipped with an LC-100 column oven and a Nelson Analytical 900 Series data station. The measurements were made by using a UV detector with absorbance at 254 nm, THF as the solvent (1 mL/min, 40 °C), two PL gel columns of 5×10^2 and 10^4 Å, and a calibration plot constructed with polystyrene standards. Elemental analysis was performed by Galbraith Laboratories.

(23) For reviews and books on molecular structure−properties correlations in molecular and macromolecular liquid crystals see: (a) Gray, G. W. *Proc. R. Soc. London, A* **1985**, *402*, 1. (b) Engel, M.; Hisgen, B.; Keller, R.; Kreuder, W.; Reck, B.; Ringsdorf, H.; Schmidt, H. W.; Tschirner, P. *Pure Appl. Chem.* **1985**, 57, 1009. (c) Gray, G. W., Ed. *Thermotropic Liquid Crystals*; Willey: New York, 1987. (d) Demus, D. *Mol. Cryst. Liq. Cryst.* **1988**, *165*, 45. (e) Demus, D. *Liq. Cryst.* **1989**, *5*, 75. (f) Weissflog, W.; Demus, D.; Diell, S.; Nitschke, P.; Wedler, W. *Liq. Cryst.* **1989**, *5*, 111. (g) Nöel, C.; Navard, P. *Prog. Polym. Sci.* **1991**, *16*, 55. (h) Gasparoux, H.; Hardouin, F.; Destrade, C.; Nguyen, H. T. *New J. Chem.* **1992**, *16*, 295. (i) Malthête, J.; Nguyen, H. T., Destrade, C. *Liq. Cryst.* **1993**, *13*, 171. (j) Donald, A. M.; Windle, A. H. *Liquid Crystalline Polymers*; Cambridge University Press: 1992. (k) Chandrasekhar, S. *Liquid Crystals*, 2nd ed.; Cambridge University Press: 1992. (l) de Gennes, P. G.; Prost, J. In *The Physics of Liquid Crystals*; De Gennes, P. E., Ed.; Oxford University Press: Oxford, 1993.

A Perkin-Elmer DSC-7 differential scanning calorimeter, calibrated with In and Zn, was used to measure the thermal transitions. Heating and cooling rates were 10 °C/min in all cases. First-order transitions (crystal−crystal, crystal−liquid crystal, liquid crystal−isotropic, etc.) were read at the maxima and minima of the endothermic and exothermic peaks, respectively. Glass transition temperatures (T_g) were read at the middle of the change in the heat capacity. All heating and cooling scans after the first heating scan were identical.

An Olympus BX40 optical polarized microscope (magnification 150×) equipped with a Mettler FP 82 hot stage and a Mettler FP 800 central processor was used to observe the thermal transitions and to verify the anisotropic textures.

X-ray diffraction experiments on liquid crystal phases of the monodendrons and dendrimers were performed using an image plate area detector (MAR Research) with a graphite-monochromatized pinhole-collimated beam and a helium tent. The samples, in glass capillaries, were held in a temperature-controlled cell. They were preoriented in a 1 T field of a heated magnetic cell.

Molecular modeling was performed with MacroModel software (Columbia University) using the MM3 force field for energy minimization on a Silicon Graphics computer.

Synthesis. 13-Hydroxy-1-(4-hydroxyphenyl)-2-(4-hydroxy-4″-p-terphenylyl)tridecane (5). **5** was obtained by the demethylation of **4** with CH_3MgI.[11] Mg (12.9 g, 0.53 mol) was placed in a 1 L three-neck flask containing 250 mL of dry Et_2O and stirred at room temperature under Ar. After adding several crystals of I_2 to initiate the reaction, CH_3I (75 g, 0.53 mol) in 250 mL of anhydrous Et_2O was added dropwise over 5 h, and stirring was continued for other 5 h until Mg was consumed completely. After **4** (25 g, 0.044 mol) was added to the reaction mixture, Et_2O was distilled and the temperature was increased to 110 °C in about 2 h. During this time, **4** dissolved in the CH_3MgI solution, and the demethylation started when bubbles occurred in the reaction mixture. The reaction temperature was raised to 140 °C and maintained for 5 h, and the melted reaction mixture became first viscous and then solid. Then the reaction was cooled with an acetone−dry ice bath, THF was added slowly to form a yellow solution, and H_2O was added dropwise until two phases separated. The organic phase was separated, and the water phase was extracted with Et_2O. The combined solution was evaporated to yield a yellow crude product which was washed with $CHCl_3$ to give a yellow pale powder. Recrystallization from toluene yielded 80.4 g (94%) of white crystals. Purity (HPLC): 99.5%. Mp: 175−175.5 °C. IR: 3600−3050 (s, OH), 3020, 2910 (s), 2840 (s), 1585 (s), 1500, 1480 (s), 1440 (s), 1360, 1230 (s), 1165, 1095, 1045, 1000, 960, 800 (s), 700 cm^{-1}. ^1H NMR (acetone-d_6, TMS, δ, ppm): 1.22 (m, 16H, $-(CH_2)_8CH_2CH_2OH$), 1.42−1.53 (m, 2H, $-CH_2CHCH_2-$monophenyl), 1.68 (m, 2H, $-CH_2CH_2-$OH), 2.84 (s, 1H, $-OH$), 2.91−2.94 (m, 3H, $-CHCH_2-$monophenyl), 3.51 (t, 2H, $-CH_2OH$, J = 6.5 Hz), 6.68 (d, 2H, ortho to the hydroxy of the monophenyl ring, J = 8.4 Hz), 6.94 (d, 4H, ortho to the hydroxy of the terphenyl ring and meta to the hydroxy of the monophenyl ring, J = 8.4 Hz), 7.27 (d, 2H, ortho to the methine of the terphenyl ring, J = 8.2 Hz), 7.56 (d, 2H, meta to the hydroxy of the terphenyl ring, J = 8.4 Hz), 7.60 (d, 2H, meta to the methine of the terphenyl ring, J = 8.0 Hz), 7.68 (s, 4H, second phenyl of the terphenyl ring), 8.08 (s, 1H, HO−monophenyl), 8.53 (s,1H, HO−terphenyl). ^{13}C NMR (acetone-d_6, δ, ppm): 26.62, 28.2, 30.25, 33.64, 36.17, 43.45, 48.55, 62.48, 115.64, 116.57, 127.13, 127.4, 127.75, 128.6, 129.17, 130.79, 132.24, 133.46, 138.74, 139.59, 140.36, 145.65, 156.25, 158.06. Anal. Calcd for $C_{37}H_{44}O_3$: C, 82.80; H, 8.26. Found: C, 82.89; H, 8.52.

Synthesis of G_1(OH) (9). 13-Hydroxy-1-(4-hydroxyphenyl)-2-(4-hydroxy-4″-*p*-terphenylyl)tridecane (**5**) (30 g, 0.056 mol) and 112 mL of 10 N NaOH were placed in a 500 mL one-neck flask equipped with a stirring bar and condenser, and the contents were stirred until a solution formed. 1-Bromo-10-undecene (26.72 g, 0.114 mol), 150 mL of *o*-DCB, and TBAH (37.96 g, 0.112 mol) were added to the flask. The reaction mixture was stirred vigorously under N_2 at 80 °C for 8 h, then it was cooled to room temperature, and 100 mL of CH_2Cl_2 was added. The organic phase was separated and washed with 100 mL of H_2O (three times), dilute HCl, and again 100 mL of H_2O (three times), and the solvent was distilled on a rotary evaporator. Then 100 mL of CH_2Cl_2 was added to dissolve the solid mixture, and the solution was poured into 2 L of CH_3OH to precipitate a light yellow powder. The crude product was purified by column chromatography (silica gel, CH_2Cl_2) to give **9** (37.6 g, 80%) as a white solid. Purity (HPLC): 99.5%. Mp: 74 °C. IR: 3560−3100 (OH), 3060, 3020, 2920 (s), 2850 (s), 1600 (s), 1540, 1510, 1485, 1460, 1290, 1245 (s), 1170, 1100, 1030, 900, 800 (s), 710 cm^{-1}. ^1H NMR ($CDCl_3$, TMS, δ, ppm): 1.21−1.52 (m, 40H, 2 $-(CH_2)_6CH_2CH{=}CH_2$ and $-(CH_2)_8CH_2CH_2OH$), 1.52−1.61 (m, 2H, $-CH_2(CH_2)_{10}OH$), 1.61−1.71 (m, 2H, $-CH_2CH_2OH$), 1.71−1.85 (m, 4H, $PhOCH_2CH_2-$ and $PhPhPhOCH_2CH_2-$), 2.06 (m, 4H, 2 $-CH_2CH{=}CH_2$), 2.83 (m, 3H, $PhCHCH_2Ph$), 3.63 (t, 2H, $-CH_2$-OH, J = 6.4 Hz), 3.90 (t, 2H, $PhOCH_2-$, J = 6.6 Hz), 4.01 (t, 2H, $PhPhPhOCH_2-$, J = 6.6 Hz), 4.96 (m, 4H, 2 $-CH{=}CH_2$), 5.72−5.92 (m, 2H, 2 $-CH{=}CH_2$), 6.75 (d, 2H, ortho to the methylene oxide of the monophenyl ring, J = 8.5 Hz), 6.95 (d, 2H, ortho to the methylene oxide of the terphenyl ring, J = 8.4 Hz), 6.99 (d, 2H, meta to the methylene oxide of the monophenyl ring, J = 8.5 Hz), 7.18 (d, 2H, ortho to the methine of the terphenyl ring, J = 8.5 Hz), 7.54 (d, 2H, meta to the methylene oxide of the terphenyl ring, J = 8.4 Hz), 7.57 (d, 2H, meta to the methine of the terphenyl ring, J = 8.5 Hz), 7.64 (s, 4H, second phenyl of the terphenyl ring). ^{13}C NMR ($CDCl_3$, δ, ppm): 25.71, 26.05, 27.56, 28.91, 29.11, 29.40, 29.51, 32.78, 33.80, 35.39, 42.91, 47.85, 63.05, 67.88, 68.06, 114.01, 114.11, 114.79, 126.59, 126.89, 127.15, 127.92, 128.20, 129.99, 132.64, 133.00, 138.11, 139.21, 139.40, 144.65, 157.21, 158.72. Anal. Calcd for $C_{59}H_{84}O_3$: C, 84.23; H, 10.06. Found: C, 83.85; H, 10.06.

Synthesis of G_1(Br) (10). To a one-neck flask cooled with an ice−water bath containing a solution of PPh_3 (10.76 g, 0.041 mol) in 100 mL of dry CH_2Cl_2 was added dropwise a solution of **G_1(OH)** (**9**) (23 g, 0.027 mol), CBr_4 (11.34 g, 0.034 mol), and 500 mL of dry CH_2Cl_2, and the mixture was stirred under N_2 for 6 h at room temperature. The solvent was evaporated until a white solid started to precipitate, and the solution was poured into 2 L of CH_3OH to precipitate 24.7 g (100%) of **10** (white powder). The compound was further purified by column chromatography (silica gel, CH_2Cl_2/hexane = 1.0/1.0) to yield 24 g (97%) of **10**. Purity (HPLC): 99.5%. Mp: 58.4 °C IR: 3060, 3020, 2920 (s), 2840 (s), 1570, 1500, 1480 (s), 1460, 1380, 1275, 1235 (s), 1170, 1100, 1030, 990, 900, 800 (s), 710 cm^{-1}. ^1H NMR ($CDCl_3$, TMS, δ, ppm): 1.21−1.52 (m, 40H, 2 $-(CH_2)_6CH_2CH{=}CH_2$ and $-(CH_2)_8CH_2CH_2Br$), 1.52−1.61 (m, 2H, $-CH_2(CH_2)_{10}Br$), 1.61−1.71 (m, 2H, $-CH_2CH_2Br$), 1.71−1.85 (m, 4H, $PhOCH_2CH_2-$ and $PhPhPhOCH_2CH_2-$), 2.06 (m, 4H, 2 $-CH_2CH{=}CH_2$), 2.84 (m, 3H, $PhCHCH_2Ph$), 3.40 (t, 2H, $-CH_2Br$, J = 6.9 Hz), 3.91 (t, 2H, $PhOCH_2-$, J = 6.6 Hz), 4.02 (t, 2H, $PhPhPhOCH_2-$, J = 6.5 Hz), 4.96 (m, 4H, 2 $-CH{=}CH_2$), 5.72−5.92 (m, 2H, 2 $-CH{=}CH_2$), 6.75 (d, 2H, ortho to the methylene oxide of the monophenyl ring, J = 8.7 Hz), 6.96 (d, 2H, ortho to the methylene oxide of the terphenyl ring, J = 8.3 Hz), 6.99 (d, 2H, meta to the methylene oxide of the monophenyl ring, J = 8.7 Hz), 7.18 (d, 2H, ortho to the methine of the terphenyl ring, J = 8.4 Hz), 7.54 (d, 2H, meta to the methylene oxide of the terphenyl ring, J = 8.3 Hz), 7.58 (d, 2H, meta to the methine of the terphenyl ring, J = 8.4 Hz), 7.64 (s, 4H, second phenyl of the terphenyl ring). ^{13}C NMR ($CDCl_3$, δ, ppm): 26.07, 27.56, 28.17, 28.75, 28.94, 29.12, 29.40, 29.66, 32.84, 33.80, 33.98, 35.44, 42.94, 47.86, 67.95, 68.12, 114.10, 114.85, 126.62, 126.92, 127.17, 127.94, 128.22, 130.01, 132.68, 133.07, 138.18, 139.20, 139.28, 139.46, 144.68, 157.29, 158.78. Anal. Calcd for $C_{59}H_{83}O_2Br$: C, 78.37; H, 9.25. Found: C, 78.41; H, 8.85.

Synthesis of G_2(OH) (11). **G_2(OH)** (**11**) was prepared from **G_1-(Br)** (**10**) (30 g, 0.033 mol), **5** (8.262 g, 16 mmol), TBAH (10.45 g, 0.031 mol), 38 mL of 10 N NaOH, 50 mL of H_2O, and 120 mL of *o*-DCB by stirring for 20 h at 80 °C. It was purified by column chromatography (silica gel, CH_2Cl_2/hexane = 1.5/1.0) to yield 21.2 g (63%) of white solid. Purity (HPLC): 99.5%. Mp: 92.0 °C. IR: 3600−3100 (OH), 3060, 3020, 2920 (s), 2850 (s), 1640, 1600 (s), 1570, 1505, 1485, 1460, 1380, 1280, 1240 (s), 1170, 1100, 1040, 990, 800 (s), 710 cm^{-1}. ^1H NMR ($CDCl_3$, TMS, δ, ppm): 1.21−1.52 (m, 96H, 4 $-(CH_2)_6CH_2CH{=}CH_2$, 2 $-(CH_2)_8CH_2CH_2O-$ and $-(CH_2)_8CH_2CH_2$-OH), 1.52−1.61 (m, 6H, $-CH_2(CH_2)_{10}OH$, 2 $-CH_2(CH_2)_{10}O-$), 1.63−1.71 (m, 2H, $-CH_2CH_2OH$), 1.71−1.85 (m, 12H, 3 $PhOCH_2CH_2-$ and 3 $PhPhPhOCH_2CH_2-$), 2.05 (m, 8H, 4 $-CH_2CH{=}CH_2$), 2.84 (m, 9H, 3 $PhCHCH_2Ph$), 3.63 (t, 2H, $-CH_2OH$, J = 7.7 Hz), 3.90 (t, 6H, 3 $PhOCH_2-$, J = 6.4 Hz), 4.01 (t, 6H, 3 $PhPhPhOCH_2-$, J = 6.4 Hz), 4.96 (m, 8H, 4 $-CH{=}CH_2$), 5.72−5.92 (m, 4H, 4 $-CH{=}CH_2$), 6.75 (d, 6H, ortho to the methylene oxide of the monophenyl ring, J = 8.3 Hz), 6.96 (d, 6H, ortho to the methylene oxide of the terphenyl ring,

J = 8.3 Hz), 6.99 (d, 6H, meta to the methylene oxide of the monophenyl ring, J = 8.3 Hz), 7.18 (d, 6H, ortho to the methine of the terphenyl ring, J = 8.3 Hz), 7.54 (d, 6H, meta to the methylene oxide of the terphenyl ring, J = 8.3 Hz), 7.57 (d, 6H, meta to the methine of the terphenyl ring, J = 8.3 Hz), 7.64 (s, 12H, second phenyl of the terphenyl ring). ^{13}C NMR ($CDCl_3$, δ, ppm): 25.72, 26.06, 27.57, 28.93, 29.12, 29.41, 29.52, 32.80, 33.80, 35.42, 42.93, 47.86, 63.08, 67.91, 68.09, 114.03, 114.80, 126.62, 126.90, 127.17, 127.93, 128.21, 130.01, 132.66, 133.02, 138.14, 139.23, 139.41, 144.68, 157.24, 158.74. Anal. Calcd for $C_{155}H_{208}O_7$: C, 85.27; H, 9.60. Found: C, 85.07; H, 9.56.

Synthesis of G_2(Br) (12). **G_2(Br)** was prepared from **G_2(OH)** (11) (18.2 g, 8.39 mmol), CBr_4 (3.467 g, 10.5 mmol), and PPh_3 (3.30 g, 12.6 mmol) in 350 mL of dry CH_2Cl_2 by stirring overnight at room temperature, and was purified by column chromatography (silica gel, CH_2Cl_2/hexane = 1.0/1.5). A white solid (17.6 g, 94%) was obtained. Purity (HPLC): 99.5%. Mp: 90 °C. IR: 3060, 3020, 2920 (s), 2840 (s), 1640, 1595 (s), 1570, 1500, 1480, 1450 (s), 1380, 1280, 1235 (s), 1170, 1100, 1040, 980, 900, 800 (s), 710 cm^{-1}. ^{1}H NMR ($CDCl_3$, TMS, δ, ppm): 1.21−1.52 (m, 96H, 4 $-(CH_2)_6CH_2CH{=}CH_2$, 2 $-(CH_2)_8CH_2CH_2O-$, and $-(CH_2)_8CH_2CH_2Br$), 1.52−1.61 (m, 6H, 2 $-CH_2(CH_2)_{10}O-$ and $-CH_2(CH_2)_{10}Br$), 1.61−1.71 (m, 2H, $-CH_2CH_2$-Br), 1.71−1.85 (m, 12H, 3 $PhOCH_2CH_2-$ and 3 $PhPhPhOCH_2CH_2-$), 2.05 (m, 8H, 4 $-CH_2CH{=}CH_2$), 2.84 (m, 9H, 3 $PhCHCH_2Ph$), 3.40 (t, 2H, $-CH_2Br$, J = 6.8 Hz), 3.91 (t, 6H, 3 $PhOCH_2-$, J = 6.6 Hz), 4.02 (t, 6H, 3 $PhPhPhOCH_2-$, J = 6.4 Hz), 4.96 (m, 8H, 4 $-CH{=}CH_2$), 5.74−5.92 (m, 4H, 4 $-CH{=}CH_2$), 6.76 (d, 6H, ortho to the methylene oxide of the monophenyl ring, J = 8.4 Hz), 6.96 (d, 6H, ortho to the methylene oxide of the terphenyl ring, J = 7.5 Hz), 7.00 (d, 6H, meta to the methylene oxide of the monophenyl ring, J = 8.4 Hz), 7.18 (d, 6H, ortho to the methine of the terphenyl ring, J = 8.3 Hz), 7.55 (d, 6H, meta to the methylene oxide of the terphenyl ring, J = 7.5 Hz), 7.58 (d, 6H, meta to the methine of the terphenyl ring, J = 8.3 Hz), 7.65 (s, 12H, second phenyl of the terphenyl ring). ^{13}C NMR ($CDCl_3$, δ, ppm): 26.05, 27.55, 28.15, 28.73, 28.91, 29.10, 29.40, 29.50, 32.81, 33.79, 34.03, 35.40, 42.91, 47.84, 67.89, 68.07, 114.01, 114.10, 114.78, 126.60, 126.89, 127.15, 127.92, 128.19, 129.99, 132.64, 133.0, 138.12, 139.21, 139.39, 144.66, 157.22, 158.72. Anal. Calcd for $C_{155}H_{207}O_6$-Br: C, 82.88; H, 9.29. Found: C, 83.10; H, 9.29.

Synthesis of G_3(OH) (13). **G_3(OH)** was prepared from **G_2(Br) (12)** (16.5 g, 7.35 mmol), **5** (2.03 g, 3.78 mmol), and TBAH (2.51 g, 7.38 mmol) in the presence of 8.6 mL of 10 N NaOH, 5 mL of H_2O, and 30 mL of *o*-DCB by stirring for 20 h at 80 °C, and was purified by column chromatography (silica gel, CH_2Cl_2/hexane = 1.0/1.0) to yield 9.4 g (51%) of a white solid. Purity (HPLC): 99.5%. Mp: 104.5 °C. IR: 3600−3200 (OH), 3060, 3020, 2920 (s), 2840 (s), 1630, 1595 (s), 1570. 1550, 1500, 1480 (s), 1455, 1380, 1270, 1240 (s), 1170, 1100, 1030, 980, 900, 800 (s), 710 cm^{-1}. ^{1}H NMR ($CDCl_3$, TMS, δ, ppm): 1.21−1.52 (m, 208H, 8 $-(CH_2)_6CH_2CH{=}CH_2$, 6 $-(CH_2)_8CH_2CH_2O-$ and $-(CH_2)_8CH_2CH_2OH$), 1.52−1.61 (m, 14H, 6 $-CH_2(CH_2)_{10}O-$ and $-CH_2(CH_2)_{10}OH$), 1.61−1.71 (m, 2H, $-CH_2CH_2OH$), 1.71−1.85 (m, 28H, 7 $PhOCH_2CH_2-$ and 7 $PhPhPhOCH_2CH_2-$), 2.06 (m, 16H, 8 $-CH_2CH{=}CH_2$), 2.83 (m, 21H, 7 $PhCHCH_2Ph$), 3.63 (t, 2H, $-CH_2$-OH, J = 6.4 Hz), 3.90 (t, 14H, 7 $PhOCH_2-$, J = 6.5 Hz), 4.01 (t, 14H, 7 $PhPhPhOCH_2-$, J = 6.4 Hz), 4.96 (m, 16H, 8 $-CH{=}CH_2$), 5.72−5.92 (m, 8H, 8 $-CH{=}CH_2$), 6.75 (d, 14H, ortho to the methylene oxide of the monophenyl ring, J = 8.2 Hz), 6.95 (d, 14H, ortho to the methylene oxide of the terphenyl ring, J = 7.2 Hz), 6.99 (d, 14H, meta to the methylene oxide of the monophenyl ring, J = 8.2 Hz), 7.18 (d, 14H, ortho to the methine of the terphenyl ring, J = 8.3 Hz), 7.54 (d, 14H, meta to the methylene oxide of the terphenyl ring, J = 7.2 Hz), 7.57 (d, 14H, meta to the methine of the terphenyl ring, J = 8.3 Hz), 7.64 (s, 28H, second phenyl of the terphenyl ring). ^{13}C NMR ($CDCl_3$, δ, ppm): 25.72, 26.07, 27.57, 28.93, 29.12, 29.42, 29.53, 32.82, 33.80, 35.43, 42.93, 47.86, 63.03, 67.91, 68.08, 114.04, 114.80, 126.61, 126.90, 127.16, 127.93, 128.21, 130.0, 132.66, 133.00, 138.13, 139.25, 139.41, 144.67, 157.24, 158.74. Anal. Calcd for $C_{347}H_{456}O_{15}$: C, 85.63; H, 9.44. Found: C, 85.82; H, 9.53.

Synthesis of G_3(Br) (14). **G_3(Br)** (**14**) was prepared from **G_3(OH)** (**13**) (5.5 g, 1.13 mmol), CBr_4 (0.474 g, 1.41 mmol), and PPh_3 (0.445 g, 1.70 mmol) in 47 mL of dry CH_2Cl_2 by stirring overnight at room temperature, and was purified by column chromatography (silica gel, CH_2Cl_2/hexane = 1.0/1.0) to yield 4.55 g (81%) of **14** as a white solid. Purity (HPLC): 99.5%. Mp: 104 °C. IR: 3060, 3020, 2920 (s), 2840 (s), 1640, 1595 (s), 1570, 1500, 1480, 1450 (s), 1380, 1280, 1230 (s), 1160, 1100, 1030, 980, 900, 800 (s), 710 cm^{-1}. ^{1}H NMR ($CDCl_3$, TMS, δ, ppm): 1.21−1.52 (m, 208H, 8 $-(CH_2)_6CH_2CH{=}CH_2$, 6 $-(CH_2)_8CH_2CH_2O-$ and $-(CH_2)_8CH_2CH_2Br$), 1.52−1.61 (m, 14H, 6 $-CH_2(CH_2)_{10}O-$ and $-CH_2(CH_2)_{10}Br$), 1.61−1.71 (m, 2H, $-CH_2CH_2$-Br), 1.71−1.85 (m, 28H, 7 $PhOCH_2CH_2-$ and 7 $PhPhPhOCH_2CH_2-$), 2.06 (m, 16H, 8 $-CH_2CH{=}CH_2$), 2.83 (m, 21H, 7 $PhCHCH_2Ph$), 3.38 (t, 2H, $-CH_2Br$, J = 6.8 Hz), 3.90 (t, 14H, 7 $PhOCH_2-$, J = 6.4 Hz), 4.00 (t, 14H, 7 $PhPhPhOCH_2-$, J = 6.2 Hz), 4.96 (m, 16H, 8 $-CH{=}CH_2$), 5.72−5.92 (m, 8H, 8 $-CH{=}CH_2$), 6.74 (d, 14H, ortho to the methylene oxide of the monophenyl ring, J = 8.0 Hz), 6.96 (d, 14H, ortho to the methylene oxide of the terphenyl ring, J = 7.4 Hz), 6.98 (d, 14H, meta to the methylene oxide of the monophenyl ring, J = 8.0 Hz), 7.17 (d, 14H, ortho to the methine of the terphenyl ring, J = 7.8 Hz), 7.53 (d, 14H, meta to the methylene oxide of the terphenyl ring, J = 7.4 Hz), 7.56 (d, 14H, meta to the methine of the terphenyl ring, J = 7.8 Hz), 7.63 (s, 28H, second phenyl of the terphenyl ring). ^{13}C NMR ($CDCl_3$, δ, ppm): 26.06, 27.57, 28.16, 28.74, 28.92, 29.12, 29.41, 29.52, 32.78, 33.80, 34.06, 35.43, 42.92, 47.86, 67.90, 68.07, 114.03, 114.10, 114.79, 126.61, 126.90, 127.16, 127.92, 128.21, 130.0, 132.65, 133.0, 138.13, 139.24, 139.41, 144.67, 157.24, 158.74. Anal. Calcd for $C_{347}H_{455}O_{14}Br$: C, 84.53; H, 9.30. Found: C, 84.16; H, 9.38.

Synthesis of G_4(OH) (15). **G_4(OH)** (**15**) was prepared from **G_3-(Br)** (**14**) (3.58 g, 0.727 mmol), **5** (0.195 g, 0.363 mmol), and TBAH (0.345 g, 1.02 mmol) in the presence of 0.73 mL of 10 N NaOH, 4.1 mL of *o*-DCB by stirring for 20 h at 80 °C, and was purified by column chromatography (silica gel, CH_2Cl_2/hexane = 1.0/1.0) to give 1.93 g (52%) of a white fluffy solid. Purity (HPLC): 99.5%. Mp: 110 °C. IR: 3600−3200 (OH), 3060, 3020, 2920 (s), 2840 (s), 1640, 1595 (s), 1570, 1500, 1480 (s), 1460, 1380, 1275, 1235 (s), 1170, 1100, 1030, 990, 900, 800 (s), 710 cm^{-1}. ^{1}H NMR ($CDCl_3$, TMS, δ, ppm): 1.21−1.52 (m, 432H, 16 $-(CH_2)_6CH_2CH{=}CH_2$, 14 $-(CH_2)_8CH_2CH_2O-$ and $-(CH_2)_8CH_2CH_2OH$), 1.52−1.61 (m, 30H, 14 $-CH_2(CH_2)_{10}O-$ and $-CH_2(CH_2)_{10}OH$), 1.61−1.71 (m, 2H, $-CH_2CH_2OH$), 1.71−1.85 (m, 60H, 15 $PhOCH_2CH_2-$ and 15 $PhPhPhOCH_2CH_2-$), 2.06 (m, 32H, 16 $-CH_2CH{=}CH_2$), 2.82 (m, 45H, 15 $PhCHCH_2Ph$), 3.61 (t, 2H, $-CH_2OH$, J = 6.4 Hz), 3.89 (t, 30H, 15 $PhOCH_2-$, J = 6.6 Hz), 4.00 (t, 30H, 15 $PhPhPhOCH_2-$, J = 6.6 Hz), 4.96 (m, 32H, 16 $-CH{=}CH_2$), 5.72−5.92 (m, 16H, 16 $-CH{=}CH_2$), 6.74 (d, 30H, ortho to the methylene oxide of the monophenyl ring, J = 8.3 Hz), 6.94 (d, 30H, ortho to the methylene oxide of the terphenyl ring, J = 8.4 Hz), 6.97 (d, 30H, meta to the methylene oxide of the monophenyl ring, J = 8.3 Hz), 7.17 (d, 30H, ortho to the methine of the terphenyl ring, J = 8.0 Hz), 7.54 (d, 30H, meta to the methylene oxide of the terphenyl ring, J = 8.4 Hz), 7.56 (d, 30H, meta to the methine of the terphenyl ring, J = 8.0 Hz), 7.63 (s, 60H, second phenyl of the terphenyl ring). ^{13}C NMR ($CDCl_3$, δ, ppm): 25.69, 26.05, 27.56, 28.90, 29.10, 29.39, 29.51, 32.76, 33.78, 35.40, 42.90, 47.83, 63.03, 67.85, 68.02, 114.00, 114.11, 114.77, 126.57, 126.85, 127.12, 127.88, 128.18, 129.98, 132.60, 133.94, 138.08, 139.18, 139.35, 144.63, 157.22, 158.71. Anal. Calcd for $C_{731}H_{952}O_{31}$: C, 85.78; H, 9.374. Found: C, 85.50; H, 9.09.

Synthesis of the G_n(D_3). **G_n(D_3)** was prepared by the esterification of the monodendron alcohol **G_n(OH)** with 1,3,5-benzenetricarbonyl trichloride.[14] To a solution of the appropriate **G_n(OH)** (3.0 equiv) and DMAP (5.11 equiv) in a minimum amount of dry CH_2Cl_2 (0.5−3.0 mL) required to form the solution in a one-neck 10 mL flask equipped with a stirring bar under N_2 was added 1,3,5-benzenetricarbonyl trichloride (1.0 equiv). Stirring was continued for 6 h, and the progress of the reaction was monitored by TLC. For the higher generations (n = 3 and 4), an excess of 1,3,5-benzenetricarbonyl trichloride (0.3 equiv) was required to completely consume the **G_n(OH)**. The reaction mixture was washed with H_2O and extracted with CH_2Cl_2 (two times). The combined solution was dried over $MgSO_4$ and evaporated to dryness. The crude white product was purified as will be described in detail in each particular case.

Synthesis of G_1(D_3) (16). To a solution of **G_1(OH)** (**9**) (0.5 g, 0.59 mmol) and DMAP (0.124 g, 1.01 mmol) in 3 mL of dry CH_2Cl_2 was added 1,3,5-benzenetricarbonyl trichloride (0.0526 g, 0.2 mmol). The reaction mixture was stirred for 6 h at room temperature and then was washed with H_2O and extracted with CH_2Cl_2 (two times), the combined organic layer was dried ($MgSO_4$), and the solvent was evaporated. The crude product was purified by column chromatography (silica gel, CH_2-

Cl_2/hexane = 2/1) to yield 0.5 g (94%) of **16** (white solid). Purity (HPLC): 99.5%. Mp: 73.3 °C. IR: 3060, 3020, 2920 (s), 2840 (s), 1860, 1715(s, CO), 1630, 1595 (s), 1575, 1500, 1480, 1460 (s), 1380, 1280, 1225 (s), 1170, 1100, 1030, 990, 960, 900, 800 (s), 735, 710, 650 cm^{-1}. ^1H NMR ($CDCl_3$, TMS, δ, ppm): 1.21−1.52 (m, 120H, 6 $-(CH_2)_6CH_2CH{=}CH_2$ and 3 $-(CH_2)_8CH_2CH_2O-$), 1.52−1.61 (m, 6H, 3 $-CH_2(CH_2)_{10}O-$), 1.61−1.71 (m, 6H, 3 $-CH_2CH_2OCO-$), 1.71−1.85 (m, 12H, 3 $PhOCH_2CH_2-$ and 3 $PhPhPhOCH_2CH_2-$), 2.06 (m, 12H, 6 $-CH_2CH{=}CH_2$), 2.82 (m, 9H, 3 $PhCHCH_2Ph$), 3.89 (t, 6H, 3 $PhOCH_2-$, J = 6.6 Hz), 4.00 (t, 6H, 3 $PhPhPhOCH_2-$, J = 6.6 Hz), 4.34 (t, 6H, 3 $-CH_2OCO-$, J = 6.6 Hz), 4.96 (m, 12H, 6 $-CH{=}CH_2$), 5.72−5.92 (m, 6H, 6 $-CH{=}CH_2$), 6.74 (d, 6H, ortho to the methylene oxide of the monophenyl ring, J = 8.4 Hz), 6.94 (d, 6H, ortho to the methylene oxide of the terphenyl ring, J = 8.4 Hz), 6.98 (d, 6H, meta to the methylene oxide of the monophenyl ring, J = 8.4 Hz), 7.16 (d, 6H, ortho to the methine of the terphenyl ring, J = 8.2 Hz), 7.52 (d, 6H, meta to the methylene oxide of the terphenyl ring, J = 8.4 Hz), 7.56 (d, 6H, meta to the methine of the terphenyl ring, J = 8.2 Hz), 7.63 (s, 12H, second phenyl of the terphenyl ring), 8.82 (s, 3H, ortho to the carbonyl of the monophenyl ring). ^{13}C NMR ($CDCl_3$, δ, ppm): 25.95, 26.04, 27.60, 28.62, 28.90, 29.11, 29.39, 29.51, 29.71, 33.79, 35.45, 42.90, 47.86, 65.83, 67.86, 68.05, 113.99, 114.11, 114.77, 126.58, 126.87, 127.13, 127.90, 128.19, 129.98, 131.43, 132.61, 132.98, 134.38, 138.10, 139.20, 139.38, 144.61, 157.20, 158.71, 165.08. Anal. Calcd for $C_{186}H_{252}O_{12}$: C, 83.36; H, 9.48. Found: C, 83.25; H, 9.68.

Synthesis of $G_2(D_3)$ (17). $G_2(D_3)$ (**17**) was prepared from $G_2(OH)$ (**11**) (0.5 g, 0.23 mmol), 1,3,5-benzenetricarbonyl trichloride (0.02 g, 0.076 mmol), and DMAP (0.048 g, 0.4 mmol) in 2.8 mL of dry CH_2Cl_2 by stirring overnight at room temperature, and was purified by column chromatography (silica gel, CH_2Cl_2/hexane = 2/1) to yield 0.4014 g (78.4%) of **17** as a white solid. Purity (HPLC): 99.5%. Mp: 96.2 °C. IR: 3060, 3020, 2920 (s), 2840 (s), 1890, 1715 (s, CO), 1630, 1595 (s), 1570, 1500, 1480, 1450 (s), 1380, 1280, 1230 (s), 1165, 1100, 1020, 990, 960, 900, 800 (s), 735, 710, 650 cm^{-1}. ^1H NMR ($CDCl_3$, TMS, δ, ppm): 1.21−1.52 (m, 288H, 12 $-(CH_2)_6CH_2CH{=}CH_2$ and 9 $-(CH_2)_8CH_2CH_2O-$), 1.52−1.61 (m, 18H, 9 $-CH_2(CH_2)_{10}O-$), 1.61−1.71 (m, 6H, 3 $-CH_2CH_2OCO-$), 1.71−1.85 (m, 36H, 9 $PhOCH_2CH_2-$ and 9 $PhPhPhOCH_2CH_2-$), 2.06 (m, 24H, 12 $-CH_2CH{=}CH_2$), 2.82 (m, 27H, 9 $PhCHCH_2Ph$), 3.89 (t, 18H, 9 $PhOCH_2-$, J = 6.4 Hz), 4.00 (t, 18H, 9 $PhPhPhOCH_2-$, J = 6.2 Hz), 4.34 (t, 6H, 3 $-CH_2OCO-$, J = 6.6 Hz), 4.96 (m, 24H, 12 $-CH{=}CH_2$), 5.72−5.92 (m, 12H, 12 $-CH{=}CH_2$), 6.74 (d, 18H, ortho to the methylene oxide of the monophenyl ring, J = 8.4 Hz), 6.94 (d, 18H, ortho to the methylene oxide of the terphenyl ring, J = 8.6 Hz), 6.98 (d, 18H, meta to the methylene oxide of the monophenyl ring, J = 8.4 Hz), 7.17 (d, 18H, ortho to the methine of the terphenyl ring, J = 8.2 Hz), 7.53 (d, 18H, meta to the methylene oxide of the terphenyl ring, J = 7.0 Hz), 7.56 (d, 18H, meta to the methine of the terphenyl ring, J = 8.6 Hz), 7.63 (s, 36H, second phenyl of the terphenyl ring), 8.82 (s, 3H, ortho to the carbonyl of the monophenyl ring). ^{13}C NMR ($CDCl_3$, δ, ppm): 26.05, 27.57, 28.62, 28.91, 29.11, 29.41, 29.52, 33.79, 35.41, 42.90, 47.85, 65.93, 67.84, 68.02, 113.98, 114.13, 114.75, 126.57, 126.86, 127.12, 127.88, 128.19, 129.98, 131.41, 132.59, 132.94, 134.36, 138.08, 139.16, 139.35, 144.62, 157.20, 158.70, 165.00. Anal. Calcd for $C_{474}H_{624}O_{24}$: C, 84.90; H, 9.38. Found: C, 84.98; H, 9.40.

Synthesis of $G_3(D_3)$ (18). $G_3(D_3)$ (**18**) was prepared from $G_3(OH)$ (**13**) (0.26 g, 0.053 mmol), 1,3,5-benzenetricarbonyl trichloride (0.006 g, 0.021 mmol), and DMAP (0.013 g, 0.01 mmol) in 1.5 mL of dry CH_2Cl_2 by stirring overnight at room temperature. 1,3,5-Benzenetricarbonyl trichloride (0.001 g, 0.0035 mmol) was added, and the reaction was continued for 6 h. The crude product was purified by column chromatography (silica gel, CH_2Cl_2/hexane = 2.5/1.0) to yield 0.131 g (50%) of **18** as a white solid. Purity (HPLC): 99.5%. Mp: 105.3 °C. IR: 3060, 3020, 2920 (s), 2840 (s), 1715 (CO), 1630, 1595 (s), 1570, 1500, 1480, 1460 (s), 1380, 1280, 1230 (s), 1170, 1100, 1020, 985, 900, 800 (s), 710, 650 cm^{-1}. ^1H NMR ($CDCl_3$, TMS, δ, ppm): 1.21−1.52 (m, 624H, 24 $-(CH_2)_6CH_2CH{=}CH_2$ and 21 $-(CH_2)_8CH_2CH_2O-$), 1.52−1.61 (m, 42H, 21 $-CH_2(CH_2)_{10}O-$), 1.61−1.71 (m, 6H, 3 $-CH_2CH_2OCO-$), 1.71−1.85 (m, 84H, 21 $PhOCH_2CH_2-$ and 21 $PhPhPhOCH_2CH_2-$), 2.06 (m, 48H, 24 $-CH_2CH{=}CH_2$), 2.82 (m, 63H, 21 $PhCHCH_2Ph$), 3.89 (t, 42H, 21 $PhOCH_2-$, J = 6.4 Hz), 3.99 (t, 42H, 21 $PhPhPhOCH_2-$, J = 6.2 Hz), 4.33 (t, 6H, 3 $-CH_2OCO-$, J = 6.4 Hz), 4.95 (m, 48H, 24 $-CH{=}CH_2$), 5.72−5.92 (m, 24H, 24 $-CH{=}CH_2$), 6.74 (d, 42H, ortho to the methylene oxide of the monophenyl ring, J = 8.4 Hz), 6.94 (d, 42H, ortho to the methylene oxide of the terphenyl ring, J = 7.2 Hz), 6.97 (d, 42H, meta to the methylene oxide of the monophenyl ring, J = 8.4 Hz), 7.16 (d, 42H, ortho to the methine of the terphenyl ring, J = 8.4 Hz), 7.52 (d, 42H, meta to the methylene oxide of the terphenyl ring, J = 7.2 Hz), 7.56 (d, 42H, meta to the methine of the terphenyl ring, J = 8.4 Hz), 7.62 (s, 84H, second phenyl of the terphenyl ring), 8.82(s, 3H, ortho to the carbonyl of the monophenyl ring). ^{13}C NMR ($CDCl_3$, δ, ppm): 26.04, 27.55, 28.61, 28.89, 29.10, 29.40, 29.51, 33.79, 35.39, 42.90, 47.83, 65.93, 67.83, 68.00, 113.97, 114.12, 114.75, 126.57, 126.85, 127.10, 127.87, 128.17, 129.97, 131.40, 132.58, 132.92, 134.33, 138.06, 139.15, 139.33, 144.61, 157.20, 158.69, 165.00. Anal. Calcd for $C_{1050}H_{1368}O_{48}$: C, 85.45; H, 9.34. Found: C, 85.44; H, 9.17.

Synthesis of $G_4(D_3)$ (19). $G_4(D_3)$ (**19**) was prepared from $G_4(OH)$ (**15**) (0.267 g, 0.026 mmol), 1,3,5-benzenetricarbonyl trichloride (0.0026 g, 0.001 mmol), and DMAP (0.0084 g, 0.068 mmol) in 1.0 mL of dry CH_2Cl_2 by stirring overnight at room temperature. Excess 1,3,5-benzenetricarbonyl trichloride (0.001 g, 0.0005 mmol) was added, and the reaction was continued for 6 h. The crude product was purified by column chromatography (silica gel, CH_2Cl_2/hexane = 1.0/1.0) to yield 0.1109 g (41%) of **19** as a white solid. Purity (HPLC): 99.5%. Mp: 108 °C. IR: 3060, 3020, 2920 (s), 2840 (s), 1715 (CO), 1630, 1595 (s), 1570, 1550, 1500, 1480, 1460 (s), 1380, 1270, 1230 (s), 1170, 1100, 1020, 985, 900, 800 (s), 650 cm^{-1}. ^1H NMR ($CDCl_3$, TMS, δ, ppm): 1.21−1.52 (m, 1296H, 48 $-(CH_2)_6CH_2CH{=}CH_2$ and 45 $-(CH_2)_8CH_2CH_2O-$), 1.52−1.61 (m, 90H, 45 $-CH_2(CH_2)_{10}O-$), 1.61−1.71 (m, 6H, 3 $-CH_2CH_2OCO-$), 1.71−1.85 (m, 180H, 45 $PhOCH_2CH_2-$ and 45 $PhPhPhOCH_2CH_2-$), 2.06 (m, 96H, 48 $-CH_2CH{=}CH_2$), 2.82 (m, 135H, 45 $PhCHCH_2Ph$), 3.89 (t, 90H, 45 $PhOCH_2-$, J = 6.6 Hz), 3.99 (t, 90H, 45 $PhPhPhOCH_2-$, J = 6.4 Hz), 4.32 (t, 6H, 3 $-CH_2OCO-$, J = 6.6 Hz) 4.95 (m, 96H, 48 $-CH{=}CH_2$), 5.72−5.92 (m, 48H, 48 $-CH{=}CH_2$), 6.74 (d, 90H, ortho to the methylene oxide of the monophenyl ring, J = 8.4 Hz), 6.94 (d, 90H, ortho to the methylene oxide of the terphenyl ring, J = 8.2 Hz), 6.96 (d, 90H, meta to the methylene oxide of the monophenyl ring, J = 8.4 Hz), 7.16 (d, 90H, ortho to the methine of the terphenyl ring, J = 8.2 Hz), 7.54 (d, 90H, meta to the methylene oxide of the terphenyl ring, J = 8.2 Hz), 7.56 (d, 90H, meta to the methine of the terphenyl ring, J = 8.2 Hz), 7.64 (s, 180H, second phenyl of the terphenyl ring), 8.82 (s, 3H, ortho to the carbonyl of the monophenyl ring). ^{13}C NMR ($CDCl_3$, δ, ppm): 26.06, 27.57, 28.61, 28.91, 29.11, 29.41, 29.52, 33.80, 35.40, 42.91, 47.85, 65.80, 67.84, 68.02, 113.98, 114.13, 114.76, 126.58, 126.86, 127.13, 127.89, 128.18, 129.99, 131.39, 132.59, 132.94, 134.36, 138.09, 139.18, 139.35, 144.63, 157.21, 158.71, 165.04. Anal. Calcd for $C_{2202}H_{2856}O_{96}$: C, 85.69; H, 9.33. Found: C, 85.04; H, 9.40.

Acknowledgment. Financial support by the National Science Foundation (Grants DMR-92-06781 and DMR-91-22227), the Office of Naval Research, the Engineering and Physical Science Research Council, U.K., and NATO (traveling grant) is gratefully acknowledged.

Supporting Information Available: Text describing the synthesis and characterization of 13-hydroxy-1-(4-methoxyphenyl)-2-(4-methoxy-4″-*p*-terphenylyl)tridecanone (**3**), 13-hydroxy-1-(4-methoxyphenyl)-2-(4-methoxy-4″-*p*-terphenylyl)-tridecane (**4**), 10-undecen-1-ol (**7**), and 1-bromo-10-undecene (**8**) and the assignments of the $^{13}C\{^1H\}$ NMR resonances obtained for 13-hydroxy-1-(4-hydroxyphenyl)-2-(4-hydroxy-4″-*p*-terphenylyl)tridecane (**5**), $G_n(OH)$ (n = 1−4), $G_n(Br)$ (n = 1−3), and $G_n(D_3)$ (n = 1−4) (9 pages). This material is contained in many libraries on microfiche, immediately follows this article in the microfilm version of the journal, can be ordered from the ACS, and can be downloaded from the Internet; see any current masthead page for ordering information and Internet access instructions.

JA952477U